

Report 73-2

January 1973

**A CASE STUDY OF APPARENT GRAVITY WAVE INITIATION
OF SEVERE CONVECTIVE STORMS**

By: L. W. Uccellini

Fausto Carlos de Almeida

Prepared for:
National Science Foundation

Grant No. GI-31278X

C. E. Anderson, Principal Investigator
D. N. Sikdar, Co-Principal Investigator

**Department of Meteorology
University of Wisconsin
Madison, Wisconsin 53706**

TABLE OF CONTENTS

ABSTRACT

Page

LIST OF SYMBOLS

Report 73-2

January 1973

SECTION I
A CASE STUDY OF APPARENT GRAVITY WAVE INITIATION OF SEVERE
CONVECTIVE STORMS

Part 1. Case Study: May 28, 1971 6
The Gravity Wave 12
The Pressure Perturbation Analysis 19
Part 4. A Comparison of the Observations with a
Numerical Model of Subsynoptic Scale
Gravity Waves 24

By: L. W. Uccellini

Prepared for:

National Science Foundation

Grant No. GI-31278X

SECTION III C. E. Anderson, Principal Investigator

The A. D. N. Sikdar, Co-Principal Investigator

SECTION IV

Summary of Results and Suggestions for Future
Research 57

APPENDIX

Filtering and Mapping Program 60

BIBLIOGRAPHY

Department of Meteorology
University of Wisconsin
Madison, Wisconsin 53706

TABLE OF CONTENTS

| | Page |
|---|------|
| ABSTRACT | iv |
| LIST OF SYMBOLS | v |
| SECTION I | |
| INTRODUCTION | 1 |
| SECTION II | |
| Part 1 Case Study: May 18, 1971 | 6 |
| Part 2 Isolating the Gravity Wave | 12 |
| Part 3 Results From the Pressure Perturbation Analysis | 19 |
| Part 4 A Comparison of the Observations With a Numerical Model of Subsynoptic Scale Gravity Waves | 34 |
| Part 5 Response of Surface Convergence Fields to the Gravity Waves | 39 |
| SECTION III | |
| The Ability of Gravity Waves to Initiate Severe Convective Storms | 45 |
| SECTION IV | |
| Summary of Results and Suggestions for Future Research | 57 |
| APPENDIX | |
| Filtering and Mapping Program | 60 |
| BIBLIOGRAPHY | 68 |

ABSTRACT

A detailed study of an outbreak of severe convective storms (May 18, 1971) was made to investigate an apparent interaction between subsynoptic scale gravity waves and the severe convective activity. An analysis of surface weather reports, radar data, surface pressure perturbations, and surface convergence revealed that the intensity of the storms pulsed with periods ranging from 2 to 4 hours; and that gravity waves, with an average period of 3 hours and trace speeds near 100 kts, were a precursor to the convective storms and apparently acted to initiate these storms. Reintensification of the convective activity, or the development of new storm cells, generally followed the passage of the trough of the gravity waves, with maximum rainfall intensity coinciding with the passage of the ridge. This proposed causal relationship was further substantiated as the observations from this case study were found to be theoretically consistent with a numerical model of subsynoptic scale gravity waves.

The gravity waves were found to exist over a much larger area than that portion of the midwest affected by the convective activity. The initiation of the convective storms occurred only where the vertical moisture distribution could support the development of such storms. The fact that some of the gravity waves originated and moved through regions void of significant thunderstorm activity indicated that mechanisms, other than the convection, would need to be isolated to determine the source of these waves.

List of Symbols

| | |
|---------------|---|
| $\omega(d)$ | Filter weight as a function of the position d |
| σ | Standard deviation of the normal curve smoothing function |
| $R_L(f)$ | Response function for low pass filter |
| $R_H(f)$ | Response function for high pass filter |
| f | Frequency |
| p' | Amplitude of pressure perturbation at surface |
| k | Wave number in the direction of propagation |
| ℓ | Wave number across axis of movement |
| $p_s(x)$ | Surface pressure |
| H_1 | Mean depth of the model layer 1 |
| ρ_0 | Surface density |
| c | Trace speed of wave |
| $w_1(x_1, z)$ | Vertical motion in the model layer 1 |
| $w_1'(z)$ | Amplitude of the vertical motion in the model layer 1 |
| W_1 | Amplitude of the vertical motion at H_1 |
| i | $\sqrt{-1}$ |
| M | $\frac{kH_1}{c\rho_0}$ |
| $D_1(x_1, z)$ | Parcel displacement in the model layer 1. |
| \bar{U} | Mean wind in the model layer 2. |
| g | Gravity |
| G | ρ_2/ρ_1 |
| N | ρ_3/ρ_1 |

| | |
|------------------------|--|
| $D_{1m}(z)$ | Amplitude of parcel displacement |
| τ | Period |
| $\overline{W}_{1m}(z)$ | Average vertical motion over 1 km sub-layers. |
| T' | Temperature of parcel |
| T | Temperature of environment |
| R | Universal gas constant |
| W_k | Net work done on parcel displaced from one level to another. |

Extensive analyses have also been undertaken to measure the mesoscale response of pressure, winds, temperature, and moisture to severe thunderstorm cells (Fujita 1963). While a great deal of knowledge has been gleaned from this period of intensive research, many aspects of convective storms are still not well understood. One aspect in particular concerns the failure to pinpoint mechanisms (other than orographic lifting and in some cases the movement of fronts) which initiate the explosive development of thunderstorms in the manner commonly observed: 1) within a short period of time, and 2) within restricted areas of synoptic scale, convectively unstable air masses.

During this period of time, the search for "triggering" mechanisms has led to some important findings. The most basic of these is the fact that mechanical energy is a necessary ingredient in the initial stage of convective storms. Rasmus (1963) showed that solar heating alone could not provide the amount of energy needed to overcome the typical inversion layer found in convectively unstable air while synoptic scale lifting would take up to twelve hours to release the instability. The combination of these two processes may be responsible for the late afternoon maximum of thunderstorm activity, but another

INTRODUCTION

Since the Thunderstorm Project (Byers and Braham 1949) a great deal of research has been undertaken to study the many aspects of severe convective storms. Both diagnostic and numerical studies have been conducted to explore the internal structure of such storms (Ludlum 1963, Fankhauser 1971, Schlesinger 1972), and to determine the synoptic situation suitable for widespread convection (Miller 1967, 1971). Extensive analyses have also been undertaken to measure the mesoscale response of pressure, winds, temperature, and moisture to severe thunderstorm cells (Fujita 1963). While a great deal of knowledge has been gleaned from this period of intensive research, many aspects of convective storms are still not well understood. One aspect in particular concerns the failure to pinpoint mechanisms (other than orographic lifting and in some cases the movement of fronts) which initiate the explosive development of thunderstorms in the manner commonly observed: 1) within a short period of time, and 2) within restricted areas of synoptic scale, convectively unstable air masses.

During this period of time, the search for "triggering" mechanisms has led to some important findings. The most basic of these is the fact that mechanical energy is a necessary ingredient in the initial stage of convective storms. Newton (1963) showed that solar heating alone could not provide the amount of energy needed to overcome the typical inversion layer found in convectively unstable air while synoptic scale lifting would take up to twelve hours to release the instability. The combination of these two processes may be responsible for the late afternoon maximum of thunderstorm activity, but another

factor must also be considered. Barber (1972) has found a significant amount of "negative energy" to exist up to the 700 mb level of tornado proximity soundings taken within 50 kilometers and one hour of tornadic storms. This fact implies that within one hour of an impending tornadic storm, the buoyancy force was acting against parcel lift in the lower portion of the troposphere and therefore inhibiting the growth of thunderstorms. Thus a significant amount of mechanical energy, applied within a one hour period, would be necessary for the severe convective storms to undergo unimpeded growth.

Other research indicates that some convective storms develop within the boundaries of small, pre-existing bands of surface convergence (Auvine 1970, Matsumoto et al. 1967, 1969 A & B, Uccellini 1971) with a magnitude of at least 10^{-4} sec^{-1} (measured in mesoscale networks, National Severe Storms Project 1963, Matsumoto and Ninomiya 1969). These convergence bands are not necessarily the results of fronts since there are cases where convective storms develop in areas removed from apparent frontal boundaries (Miller 1967, Auvine 1970, Paine 1971). Even along cold fronts strong isolated pockets of convergence mark the regions in which most of the severe storms are restricted (Uccellini 1971). It is apparent therefore that other mechanisms besides the general movement of fronts must be active to produce the isolated convergence zones associated with midwestern convective systems. And as stated before, these same mechanisms must also be capable of providing the mechanical energy needed for the initiation of such storms.

In 1950 Morris Tepper proposed that gravity waves, which are reflected at the surface by a pressure jump, could effectively lift

the lowest layers of the atmosphere and cause the development of squall lines in convectively unstable air. An exhaustive analysis of pressure traces in the midwest prior to and after the development of squall lines seemed to prove Tepper's contention (Tepper 1954). But the work done by Fujita (1955) which showed that the thunderstorm high was a result of evaporative cooling in the downdraft cast some doubt upon the pressure jump theory. Fujita concluded:

"This intense system of storms was indicated before a pressure surge line was organized. This suggests the futility of seeking a "trigger" mechanism in the pressure field at the initial stages."

It is odd however, that Fujita and others (e.g. Stadjuhar 1970) chose to ignore the dry pressure jump lines which were analyzed prior to any squall line development and along which squall lines were later formed (Tepper 1954). The absolute tone in Fujita's conclusion may also be the reason why so little effort was expended in isolating triggering mechanisms for thunderstorms until the late sixties.

It was at this time that Matsumoto and Ninomiya noted a peculiar behavior in the surface convergence fields of both summer and winter convective storms in western Japan. The magnitude of the convergence fields as well as the intensity of the storms, as reflected by precipitation rates and surface winds, pulsed with a three hour period (Matsumoto et al. 1969 A & B). Uccellini (1971) observed the same pulsating characteristic in a study of convective storms in the mid-western region of the United States. Surface convergence fields and the convective storms associated with them pulsed in intensity with periods ranging from 2.5 to 5 hours. One case study, commenced prior to any thunderstorm activity, showed that the convergence zone was

pulsating well before the convective activity developed. The magnitude of the convergence was no greater after the thunderstorms formed, nor was the pulsating nature altered (Uccellini 1971). This indicated that an external factor was responsible for this behavior and not the thunderstorms themselves. Further evidence for a long period oscillation is offered by Ninomiya (1969). He found that a series of disturbances with a period of two to four hours was associated with the severe convective activity of April 23, 1968 in the eastern third of the United States. These disturbances moved at a rate of 60 to 90 kts and were clearly illustrated by hourly surface observations such as pressure, winds, and rainfall rates. In this case, however, it is not clear if the individual moving systems varied in intensity, as was determined by Matsumoto and by Uccellini, or if the wave length of the disturbances was such that particular locations would be affected every two to four hours.

In the case studies noted above (Tepper 1950, 1954, Matsumoto et al. 1969 A & B, Ninomiya 1969, Uccellini 1971), the gravity wave was offered as the mechanism responsible for the periodic behavior of the convergence fields and of the convective storms themselves. Matsumoto and Ninomiya (1967) went one step further by stating that gravity waves activated mesoscale surface convergence capable of initiating convective snow squalls in western Japan. Yet in none of these studies was it clearly demonstrated that the pressure and convergence oscillations are related, nor was it proved that gravity waves are capable of providing the mechanical lift needed for the initiation of such storms. Diagnostic studies of gravity waves have been presented (Tepper 1951, Brunk 1949, Eom 1972) which proved that these waves could move great

distances at speeds up to 100kts and be responsible for an increase in middle and low level clouds. But no attempt has been made to prove that gravity waves are a precursor to, or are in fact a triggering mechanism of convective storms.

It is thus the purpose of this thesis to relate gravity wave activity, as illustrated by surface pressure perturbations, to the pulsating nature of convective systems. It will also be shown that gravity waves with subsynoptic scale features are indeed capable of providing the mechanical lift necessary to initiate the development of thunderstorms which ultimately lead to heavy rainfall, severe hail and windstorms, and even tornadoes. To accomplish this, an extensive diagnostic study of a storm system which developed in the midwestern region of the United States was undertaken. The results of this study are presented in the following sections. A brief description of the synoptic scale circulation is followed by a subsynoptic scale analysis of the apparent gravity wave activity. A causal relationship between the gravity wave, pulsating convergence fields, and the development of thunderstorms is then presented. Finally, a check with the numerical model derived by Eom (1972) is made to determine if the observed relationships are consistent with the theoretical aspects of the problem, and to determine if the waves are in fact capable of releasing the convective instability.

"May 17th - 18th a night of repeated numerous severe thunderstorms, hail and damaging winds southeast of Cape-Orde county line. Some sites reported two or three storms several hours apart..." (Storm Data 1971)

The storms in Iowa displayed the same behavior. A two to four hour period, both in the intensity of the storms and in the pressure traces,

Section II Part 1

Case Study: May 18, 1971

From the late afternoon of May 17th through May 18th, a developing cyclone in the midwest was the dominant feature on the synoptic maps (Figure 1). A stationary front stretched from Kansas, across Iowa, and into Wisconsin for a thirty hour period with the cyclone developing in northwestern Missouri by 0000GMT, May 19th. The 500mb charts (Figure 2) show the trough associated with the developing storm moving from the southwest quadrant of the country into the central region, where the cyclone finally developed.

An abundant amount of moisture moved northward from the Gulf of Mexico within a low level jet (Figure 3) as strong jet streaks at the 500mb level (Figure 2) moved over the frontal zone from the south-southwest. These features are signs of impending severe thunderstorms (Miller 1967) and led meteorologists in the National Severe Storm Forecast Center in Kansas City, Missouri to post numerous severe thunderstorm and tornado watches throughout the region for the night of the 17th and the afternoon and evening of the 18th of May (Figure 3).

The thunderstorms which developed during this period displayed the characteristics of the pulsating convective systems described by Uccellini (1971). The description of the storms in southeastern Nebraska by the state's climatologist illustrates this behavior:

"May 17th - 18th a night of repeated numerous severe thunderstorms, hail and damaging winds southeast of Gage-Otoe county line. Some sites reported two or three storms several hours apart..." (Storm Data 1971).

The storms in Iowa displayed the same behavior. A two to four hour period, both in the intensity of the storms and in the pressure traces,

was quite apparent (Figure 4). In fact, there seemed to be a consistent relationship between the pressure oscillation and the onset of the storms. A sharp pressure fall would be followed by the onset of intense convective storms and a subsequent pressure rise. The stationary nature of the entire synoptic system allowed for regions to experience this fluctuating pattern for an extended period of time.

A detailed analysis of the pressure field using altimeter settings from FAA and National Weather Service stations revealed that subsynoptic scale depressions were in fact moving through Iowa and seemed to be associated with the periodic behavior of the thunderstorms. Figure 5 illustrates one such disturbance which moved through Iowa and into Wisconsin at a speed of 100 knots. The nature and celerity of this depression indicate that it was a gravity wave, much like those observed by Matsumoto (1967) and Eom (1972).

While this gravity wave was quite apparent, others may go unnoticed in this type of analysis. For example, note how the pressure gradient over southeastern Nebraska shifted north and south. This behavior could be due to gravity waves, although it is not obvious from the maps in Figure 5. The subsynoptic scale waves may also be obscured by the developing cyclone in Kansas and Missouri.

Since the gravity waves could be obscured by the synoptic scale features, it was decided to filter the pressure traces from the midwest, and therefore isolate the short term fluctuations due to the gravity waves from the synoptic trends. The method by which this was done and the results obtained are presented in the following sections.

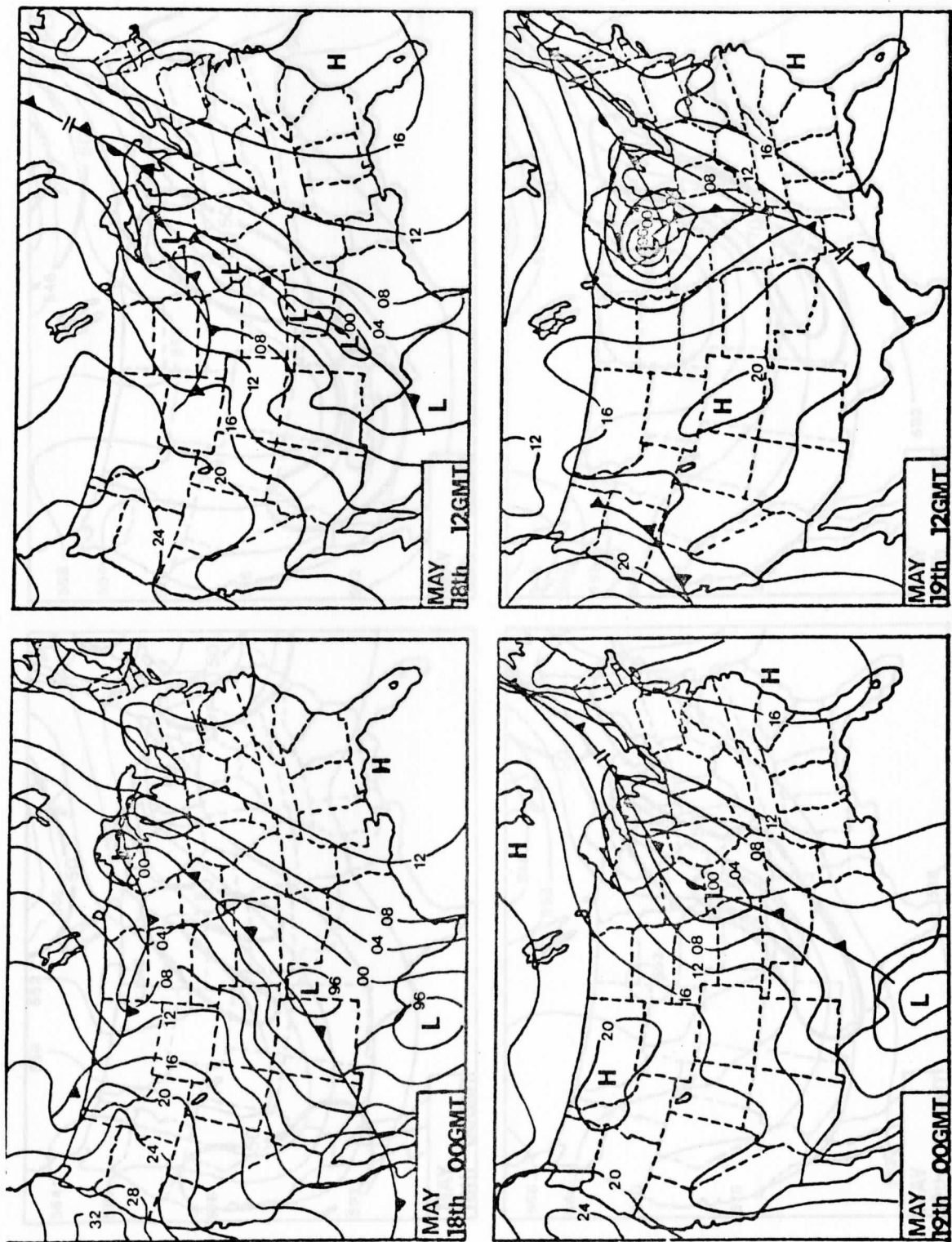


Figure 1. Surface isobaric analysis (mb) for May 18, 1971 (0000 GMT, 1200 GMT) and May 19, 1971 (0000 GMT, 1200 GMT).

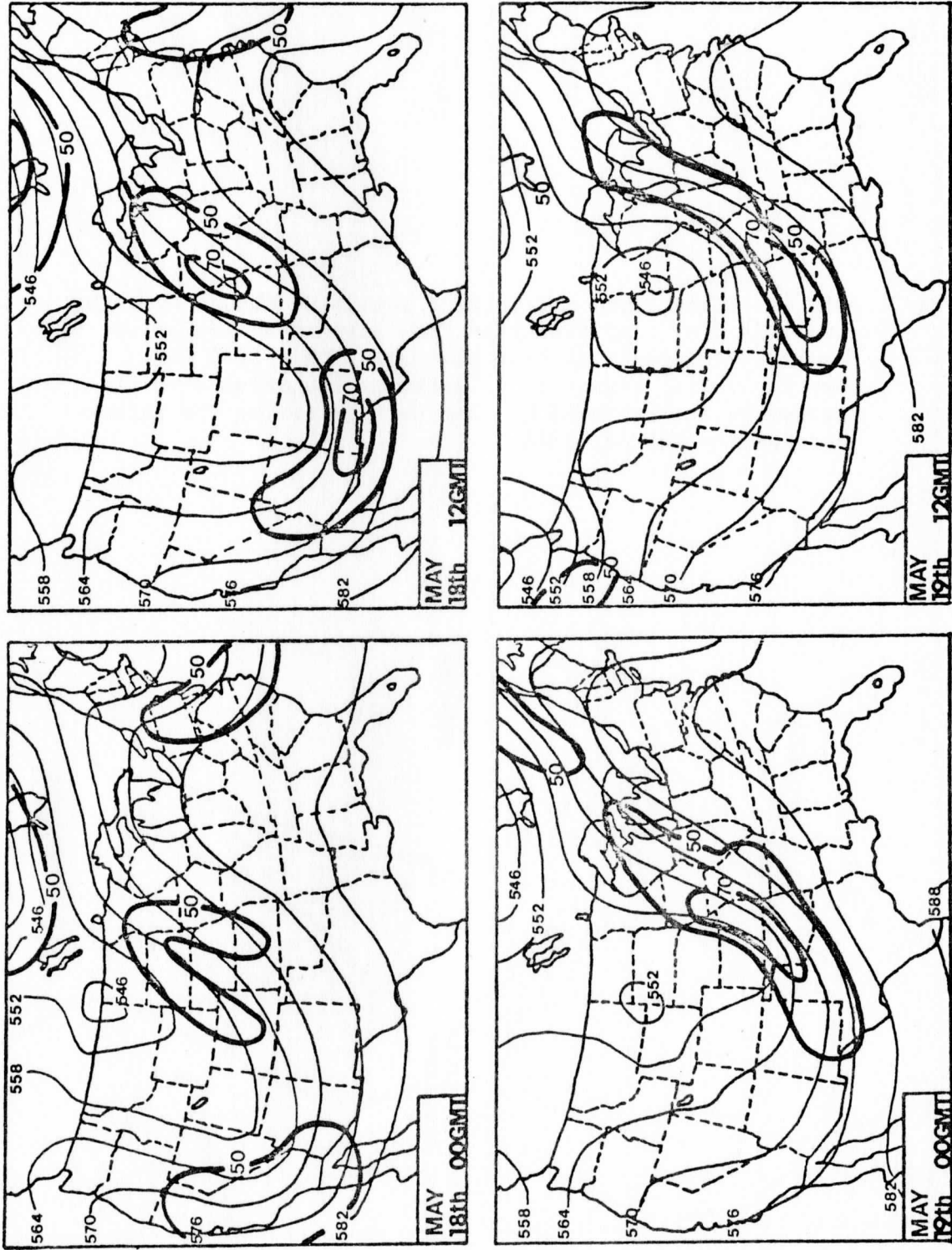


Figure 2. 500 mb height (gpm; with 552 equal to 5520 gpm)——, and isotach (kts.)—— analyses for May 18, 1971 (0000 GMT, 1200 GMT) and May 19, 1971 (0000 GMT, 1200 GMT).

Figure 3. 850 mb height (gpm) and isotach analysis, 850 mb dewpoint analysis ($^{\circ}$ c), and Showalter Stability Index (negative numbers represents an unstable region) for 1200 GMT, May 18, 1971. Figure 3D illustrates the tornado watches issued by the National Weather Service during the afternoon of the May 18, 1971.

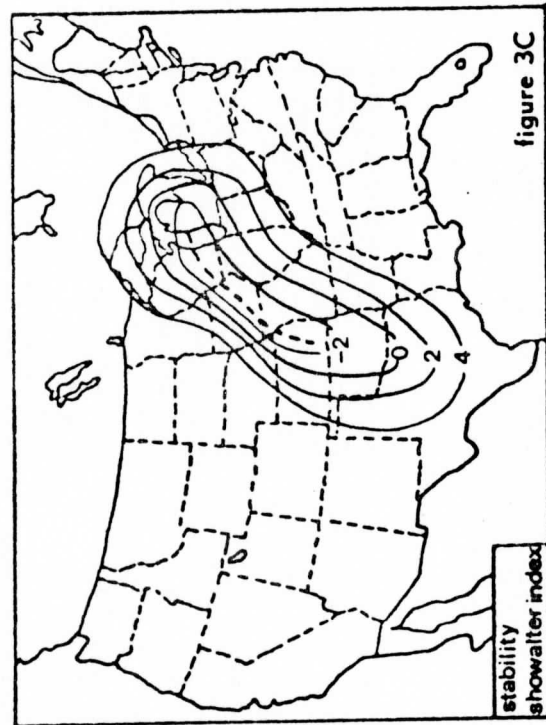
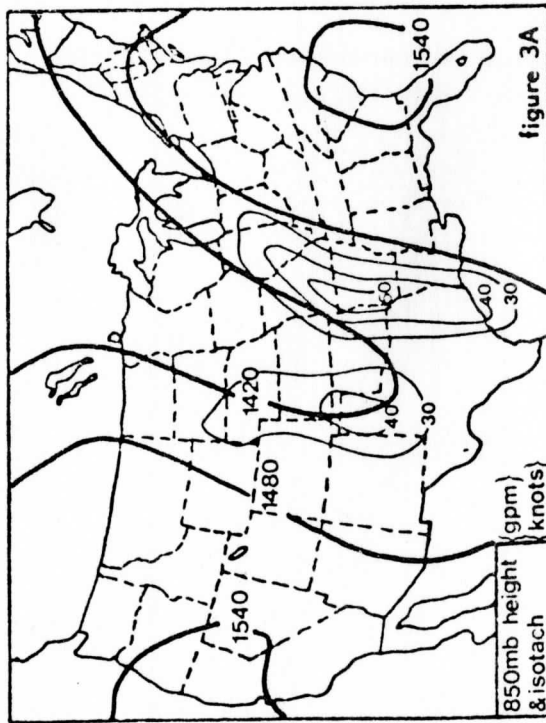
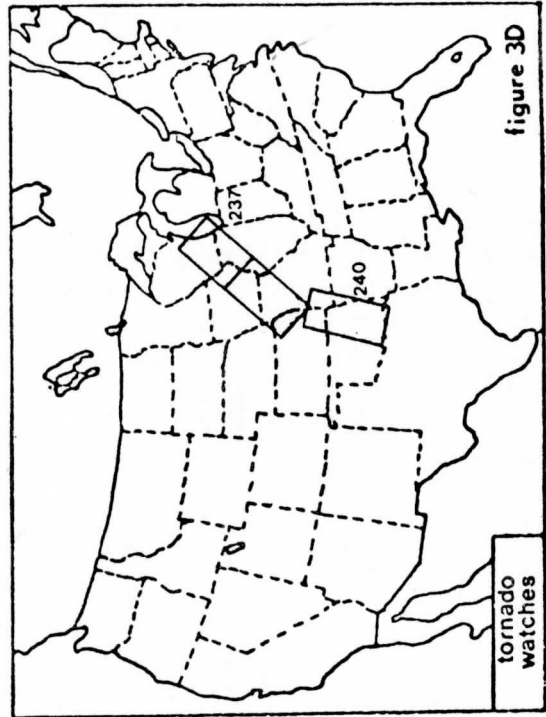
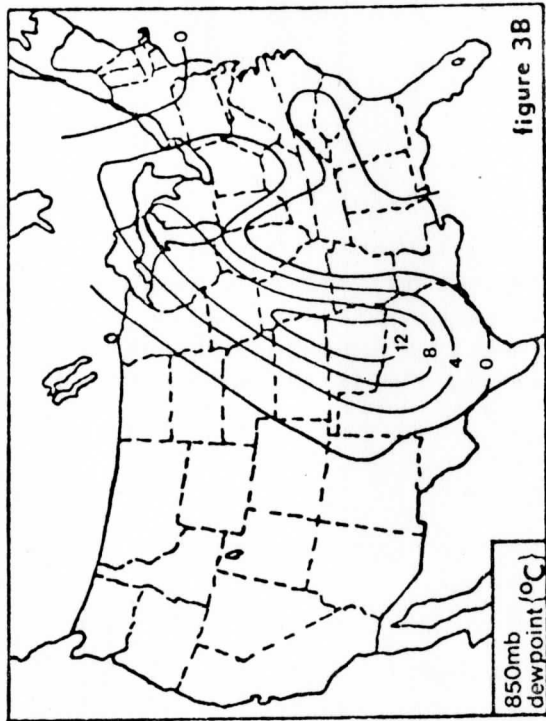


Figure 3.

Figure 4. Surface convergence for east-central Iowa (10^{-5} sec^{-1}), pressure trace for Cedar Rapids, Iowa (inches of mercury). Storm Data illustrates weather conditions near Cedar Rapids: R - (light thundershower), R (moderate thundershower) R + (heavy thundershower), \dot{v} - (light shower) V (tornado).

Figure 5. Surface isobaric analysis, using altimeter settings (inches of mercury, 58 = 29.58 in. of Hg.) for May 18, 1971, 1700 GMT through 2000 GMT.

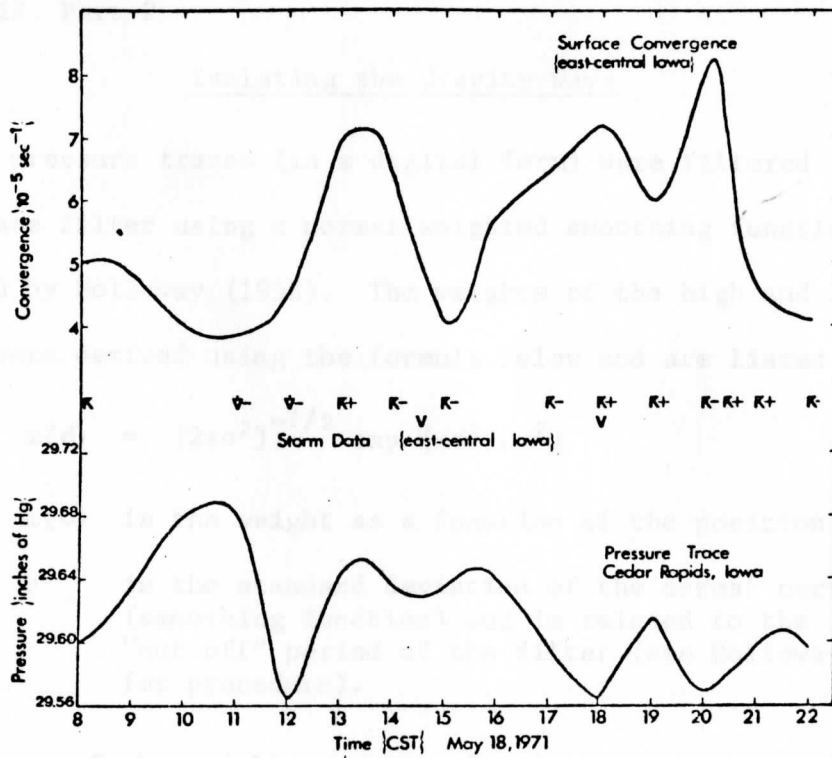


Figure 4.

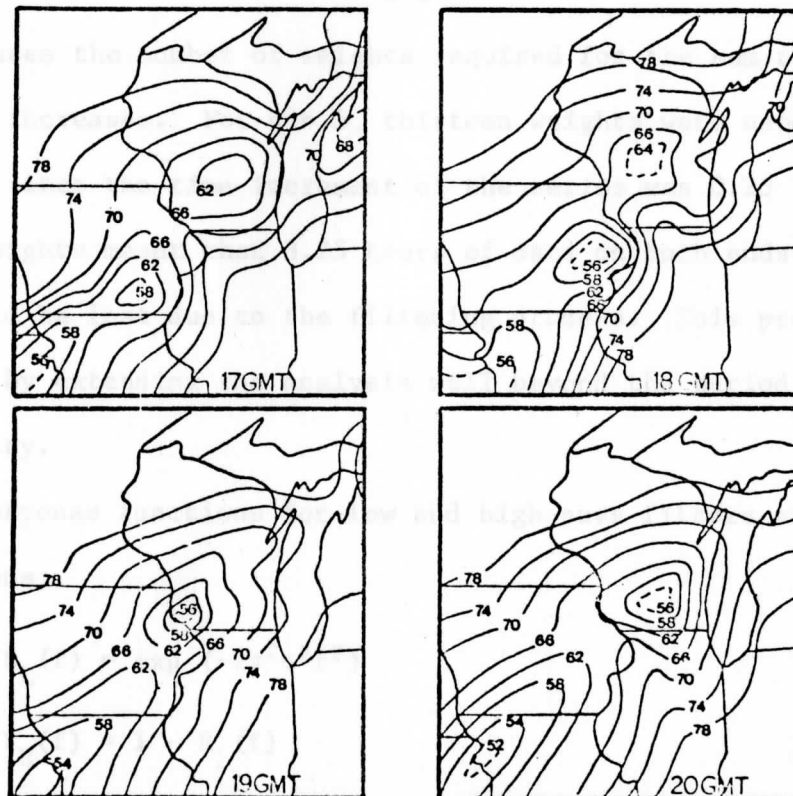


Figure 5.

Section II Part 2

Isolating the Gravity Wave

The pressure traces (in a digital form) were filtered through a band pass filter using a normal weighted smoothing function as was described by Holloway (1958). The weights of the high and low pass filters were derived using the formula below and are listed in Table 1.

$$\omega(d) = (2\pi\sigma^2)^{-1/2} \exp(-d^2/2\sigma^2)$$

$\omega(d)$ is the weight as a function of the position d .

σ is the standard deviation of the normal curve (smoothing function) and is related to the "cut off" period of the filter (see Holloway for procedure).

The sum of the weights must equal unity so as not to alter the mean value of the series, where:

$$\text{sum of weights} = \omega_0 + 2 \sum_{i=1}^N \omega_i \quad (N = \text{number of weights}).$$

As σ increases the number of weights required for the sum to equal unity also increases. For $\sigma = 5$, thirteen weights were needed for unity, and since the time increment of the series was 0.25 hours, the thirteen weights meant that 3.25 hours of data on both ends of the time series would be lost due to the filtering process. This problem was alleviated by extending the analysis well beyond the period of obvious wave activity.

The response functions for low and high pass filters are given by the equations:

$$R_L(f) = \exp(-2\pi^2\sigma^2f^2)$$

$$R_H(f) = 1 - R_L(f)$$

$R_L(f)$ is the response function for low pass filter

$R_H(f)$ is the response function for high pass filter

f is frequency

σ is the standard deviation of the normal curve smoothing function

For this study $\sigma = 5$ for the high pass filter and $\sigma = 1$ for the low pass filter.

The "cut off" periods are defined to be those periods at which $R(f) = 0.9$ for the high pass filter and $R(f) = 0.1$ for the low pass filter (check Holloway for procedure). The cut off periods are marked on Figures 6a and 6b which show the response function of the high and low pass filters used together to form the band pass filter (Figure 6c). The response function for the band pass filter rapidly approaches zero as f decreases from 0.2 cycles/hour. Therefore the low frequency waves representing synoptic scale trends are effectively eliminated. The waves having the observed two to four hour periods are passed through this filter with a slight reduction in their amplitude (since $R(f)$ is less than one). The response function gradually decreases as f increases from 0.4 cycles/hour. The high frequency waves are therefore filtered out, thus lessening the effects of individual storm cells on the pressure perturbations.

Figure 7 illustrates the success of this filter. The original pressure trace from Madison, Wisconsin (Figure 7a) was initially reduced to the pressure perturbation trace (Figure 7b) using the high pass filter ($\sigma = 5$). At this point the trend toward higher pressure during the first half of the time period and toward lower pressure

TABLE I **Weights for the High and Low Pass Filters**

| Point (d) | High Pass | | Low Pass | |
|-----------|-------------|--|-------------|---|
| | $\omega(d)$ | $\sigma = 5.0$ | $\omega(d)$ | $\sigma = 1.0$ |
| 0 | | .030 | | .399 |
| 1 | | .079 | | .242 |
| 2 | | .074 | | .054 |
| 3 | | .067 | | .004 |
| 4 | | .058 | | |
| 5 | | .049 | | |
| 6 | | .039 | | |
| 7 | | .030 | | |
| 8 | | .022 | | |
| 9 | | .016 | | |
| 10 | | .011 | | |
| 11 | | .007 | | |
| 12 | | .005 | | |
| 13 | | .003 | | |
| | | $\omega_0 + 2 \sum_{t=1}^{13} \omega(d) = 1$ | | $\omega_0 + 2 \sum_{t=1}^3 \omega(d) = 1$ |

during the last half is eliminated in Figure 7b. This perturbation trace, which has the synoptic trends filtered out, was then further smoothed using the low pass filter ($\sigma = 1$) as is shown in Figure 7c. The elimination of high frequency disturbances is reflected by the disappearance of the sharp fluctuation near 0900CST. Note also that the amplitudes of the resultant perturbation trace (Figure 7c) are reduced because of the low pass filter ($\sigma = 1$). This smoothed perturbation trace represents the gravity waves which passed through southern Wisconsin. The negative values represent the trough of the waves while the positive values represent the ridge.

Some deficiencies are inherent within this method of analysis and should be considered before evaluating the results of this work. First of all the amplitude of the waves is reduced by at least 0.3mb because of the unavoidable imperfections of the filter:

- 1) $R(f)$ is less than one in the two to four hour range indicating that part of the gravity wave is itself being filtered out.
- 2) The lack of sharp cut offs in $R(f)$ at the desired frequencies causes further reduction in the amplitude within the range of the gravity waves.

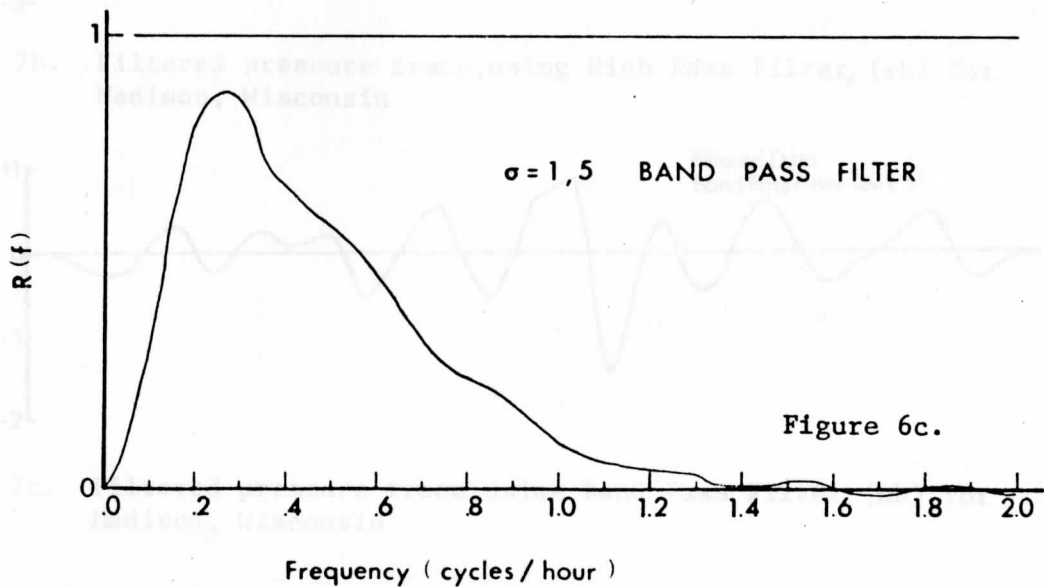
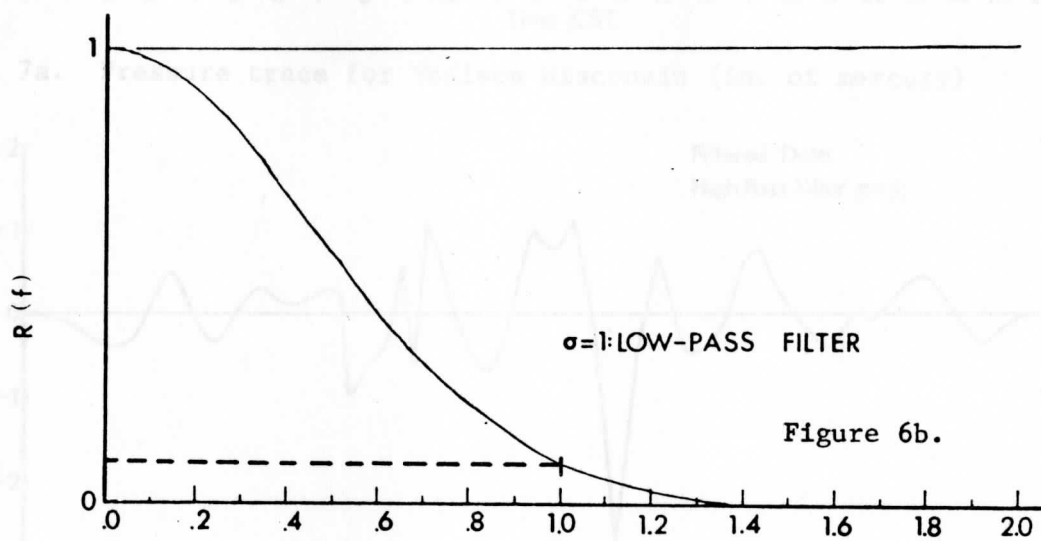
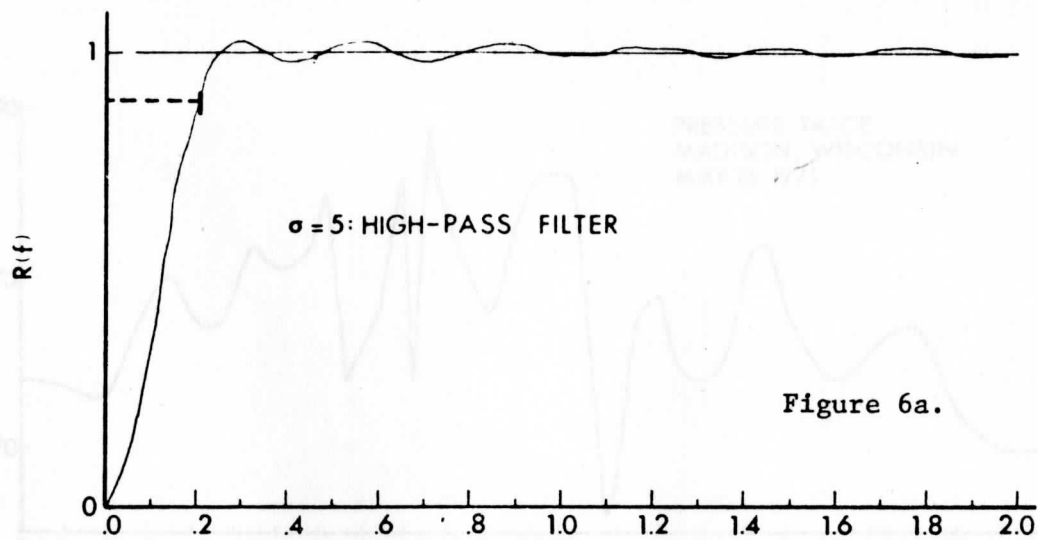
Secondly, the nonuniformity of the station density (Figure 8) could cause spatial aliasing of the perturbation values. Therefore the maximum and minimum values may pass between reporting stations and evade detection. This problem is especially acute in western Iowa, central Wisconsin, and over the Great Lakes.

The entire analysis included the filtering of over 120 pressure traces from stations throughout the midwest (Figure 8). Maps of the perturbation values were then plotted and analyzed every fifteen minutes. The fifteen minute interval between maps helped to maintain

Figure 6a. Response function for the High Pass Filter. The "cut off" period (see text) is marked on graph
 $f = .2$ cycles/hours $R(f) = .90$ "cut off" period = 5 hrs.

Figure 6b. Response function for the Low Pass Filter. The "cut off" period (see text) is marked on graph
 $f = 1.0$ cycles/hour $R(f) = .10$ "cut off" period = 1 hr.

Figure 6c. Response function for the Band Pass Filter.



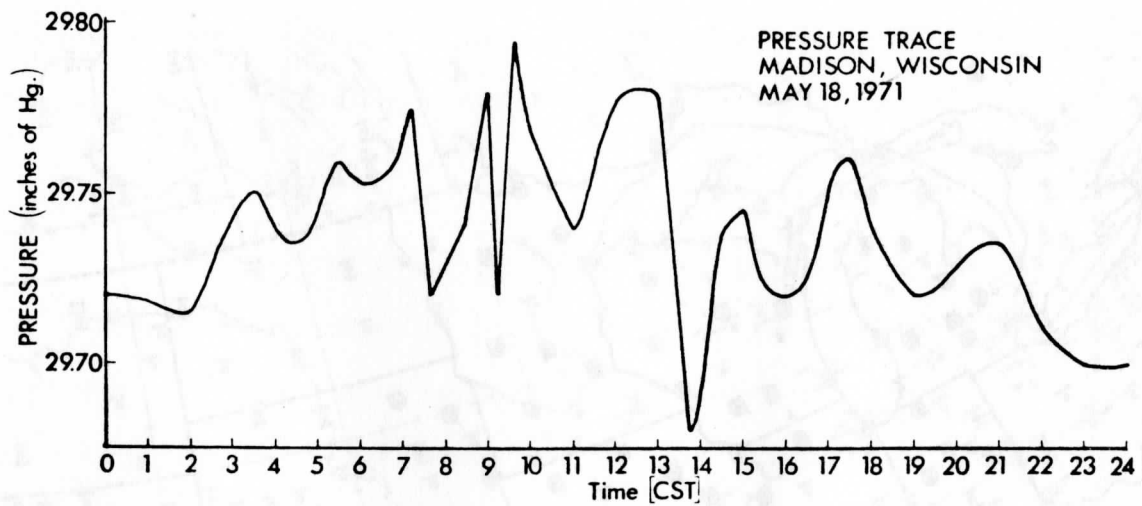


Figure 7a. Pressure trace for Madison Wisconsin (in. of mercury)

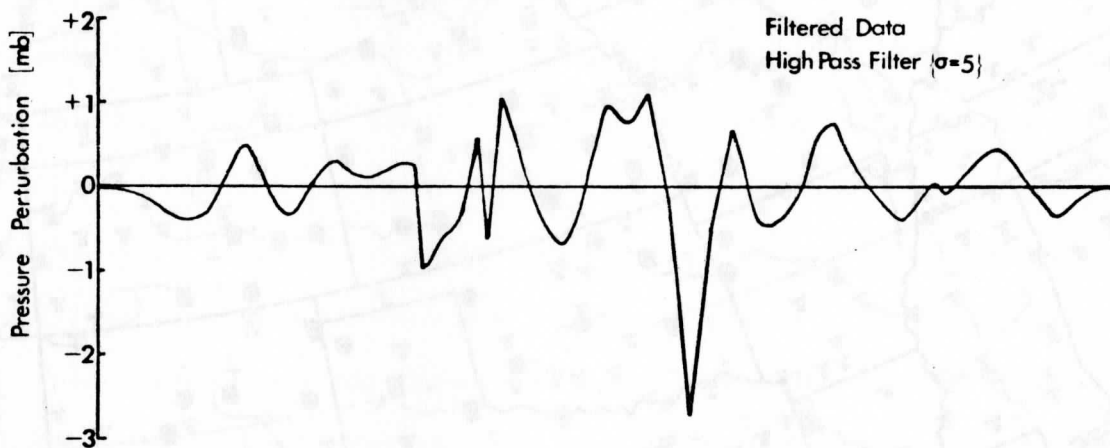


Figure 7b. Filtered pressure trace, using High Pass Filter, (mb) for Madison, Wisconsin

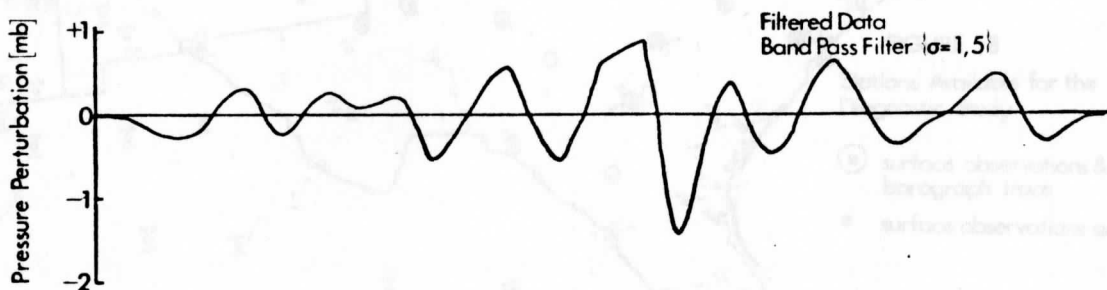


Figure 7c. Filtered pressure trace, using Band Pass Filter, (mb) for Madison, Wisconsin

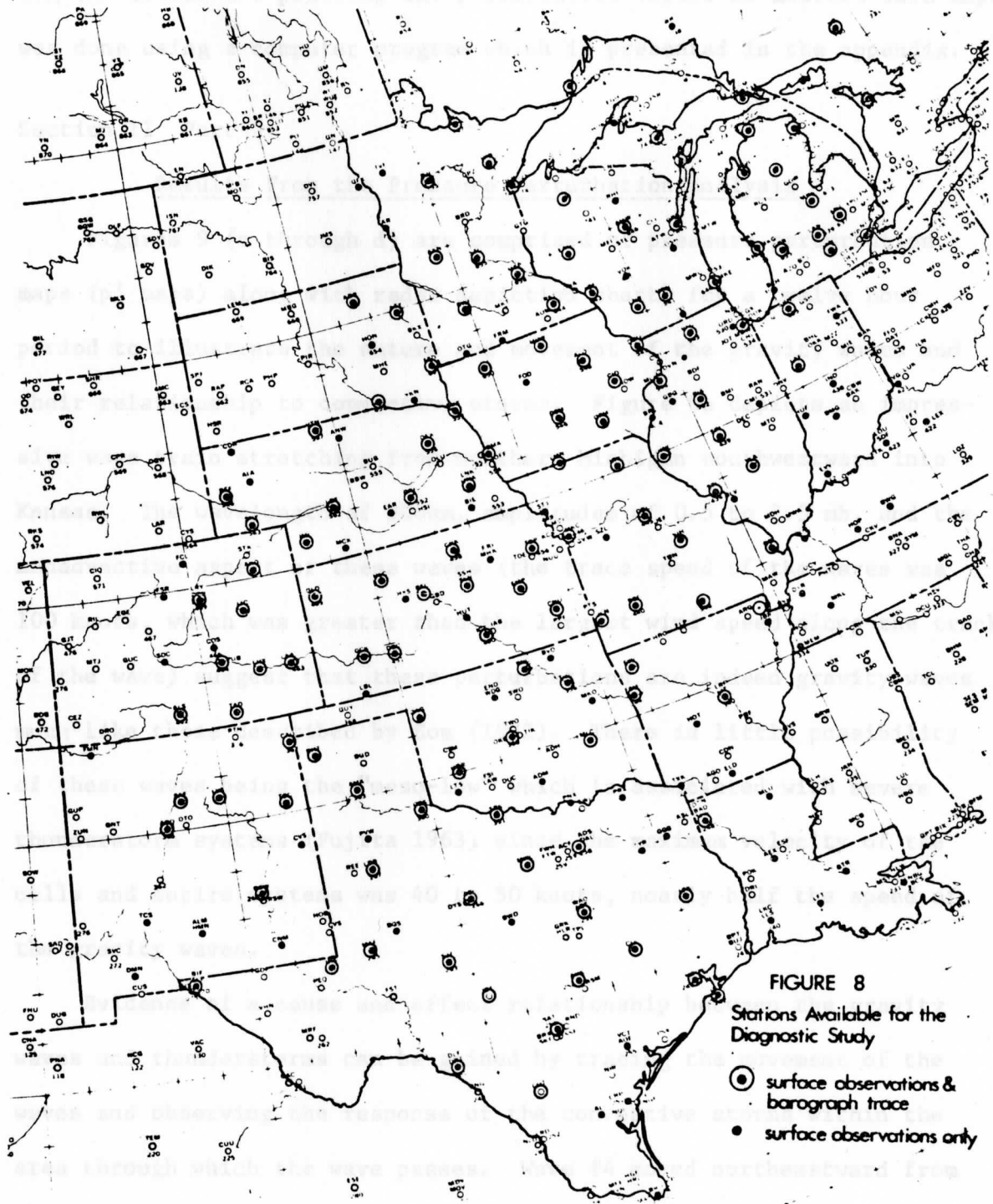


FIGURE 8
Stations Available for the
Diagnostic Study

- surface observations & barograph trace
- surface observations only

the continuity in the analysis, and therefore made it easier to identify and trace the movement of the gravity waves. The massive job of filtering the traces and plotting the perturbation values on midwest base maps was done using a computer program which is presented in the appendix.

Section II Part 3


Results From the Pressure Perturbation Analysis

Figures 9 (a through d) are comprised of pressure perturbation maps (p' maps) along with radar depiction charts for a twelve hour period to illustrate the nature and movement of the gravity waves and their relationship to convective storms. Figure 9a depicts an impressive wave train stretching from northern Michigan southwestward into Kansas. The wavelength of 300km, amplitudes of 0.5 to 2.5 mb, and the nonadvective aspect of these waves (the trace speed of the waves was 100 knots, which was greater than the largest wind speed along the track of the wave) suggest that these perturbations are indeed gravity waves much like those described by Eom (1972). There is little possibility of these waves being the "meso-low" which is associated with severe thunderstorm systems (Fujita 1963) since the maximum velocity of the cells and entire systems was 40 to 50 knots, nearly half the speed of the gravity waves.

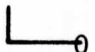
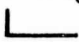
Evidence of a cause and effect relationship between the gravity waves and thunderstorms can be gained by tracing the movement of the waves and observing the response of the convective storms within the area through which the wave passes. Wave #4 moved northeastward from Kansas and Nebraska into northern Iowa and southwestern Wisconsin (Figures 9a, b, c). Note that the wave speed in this case was 100

Figure 9a. Pressure perturbation analysis and radar depiction maps for May 18, 1971.

Pressure perturbation analysis: analyzed at intervals of .50 mb, with $p' = 0$ indicated by heavy dashed line. The light dashed line indicates an interval of .25 mb. Negative p' field indicated by L. Positive p' field indicated by H.

Radar depiction maps: Area of rainfall outlined by scalloped lines squall lines indicated by narrow rectangle . Maximum cell height reported is also included (e.g. 400 = 40,000 feet). The legend below should be used to interpret the radar maps.

Type of storm (intensity)/(intensity change) (area coverage)

| | | |
|------------------|---|---|
| Type of Storm | RW | rainshower |
| | TRW | thundershower |
| Intensity | (-) | light |
| | () | moderate |
| | (+) | heavy |
| | (++) | very heavy |
| Intensity change | - | decreasing |
| | NC | no change |
| | + | increasing |
| | NEW | new cells developing within last hour |
| Area coverage | ○ | .1 to .5 coverage |
| | ◐ | .6 to .9 coverage |
| | ● | over .9 coverage . . . |
| Wind barbs | | indicates either area movement or cell movement |
| |  | cell movement |
| |  | area movement |

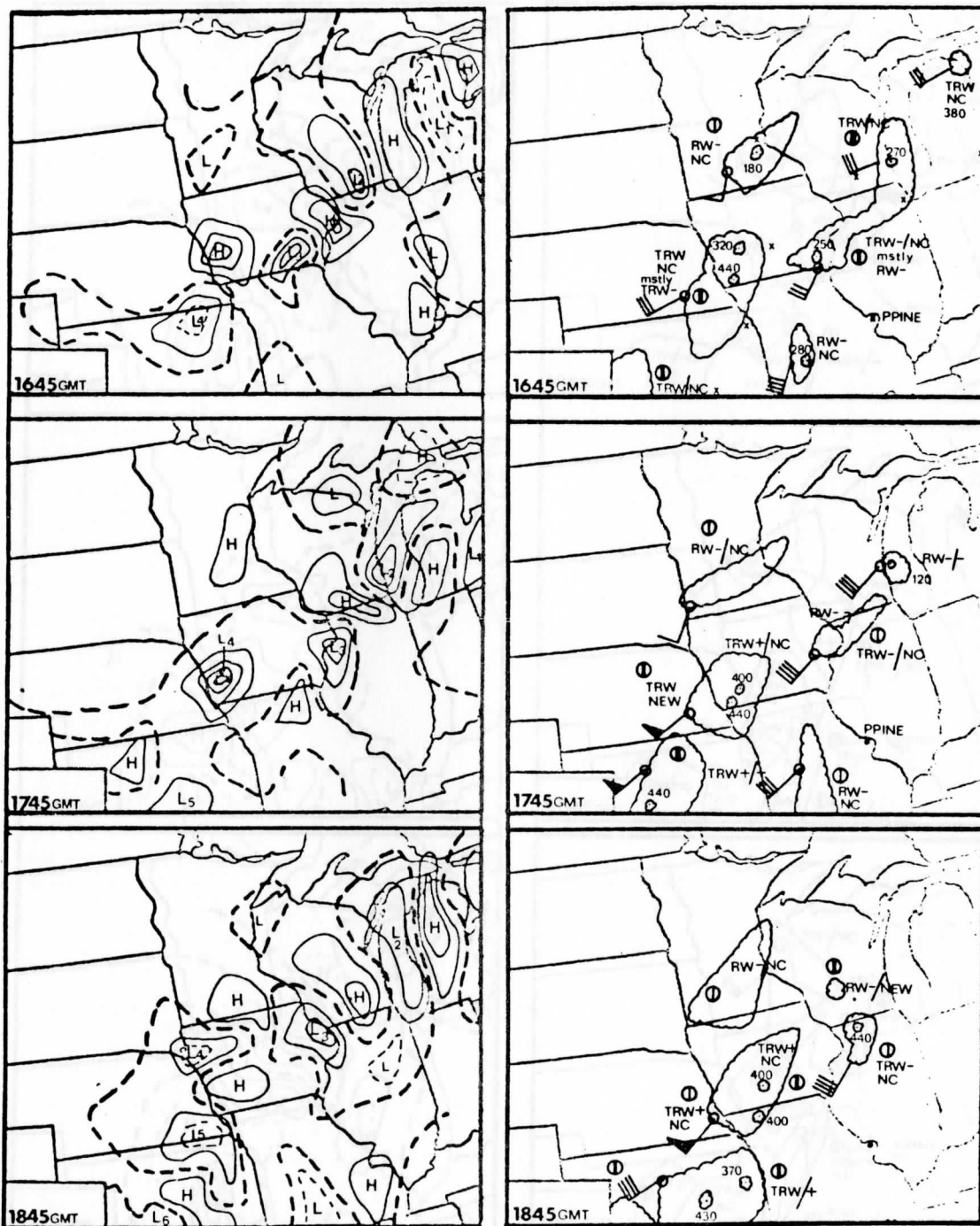


Figure 9a.



Figure 9b. Pressure perturbation and radar depiction analyses. See Figure 9a for entire legend.

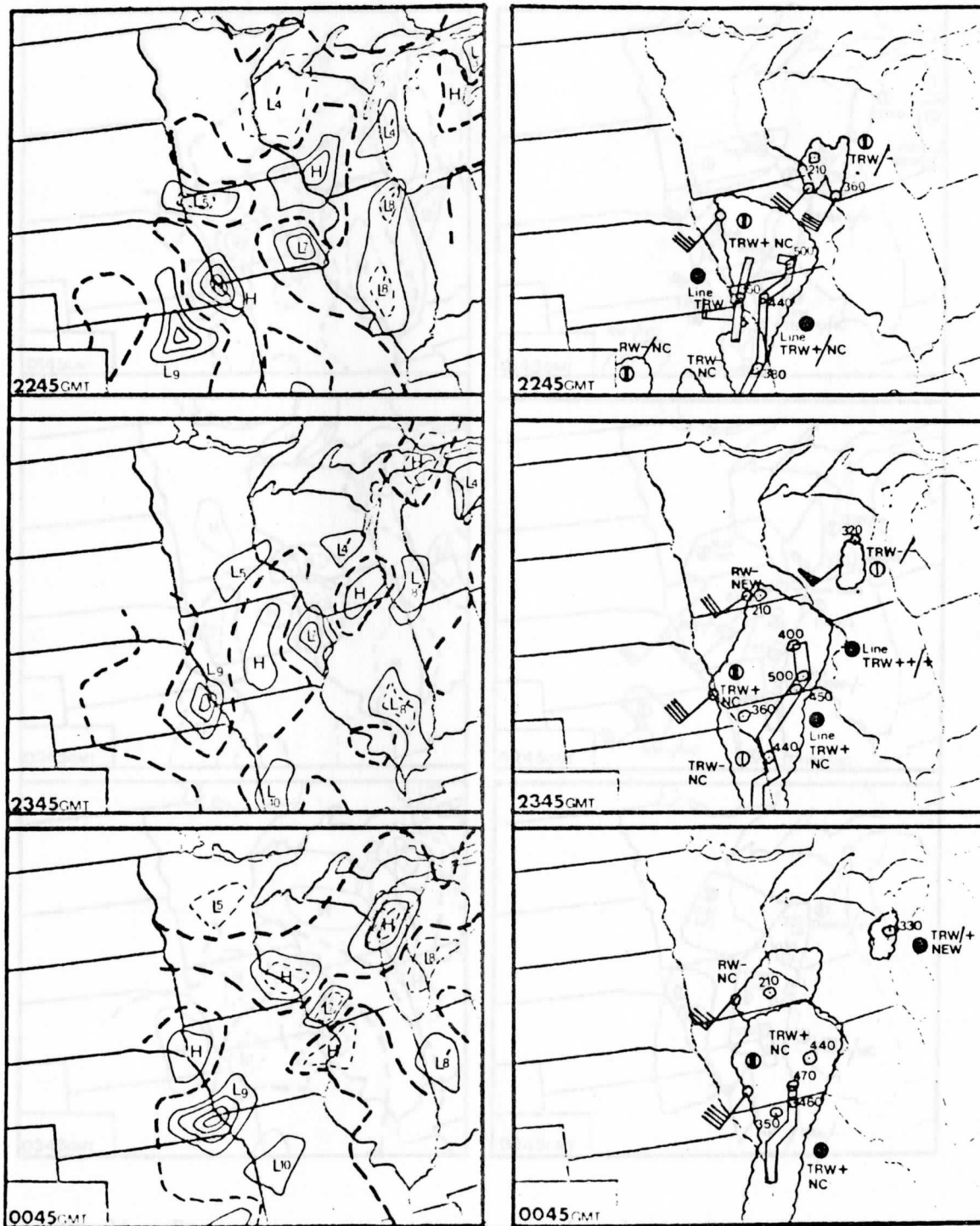


Figure 9c. Pressure perturbation and radar depiction analyses. See Figure 9a for entire legend.

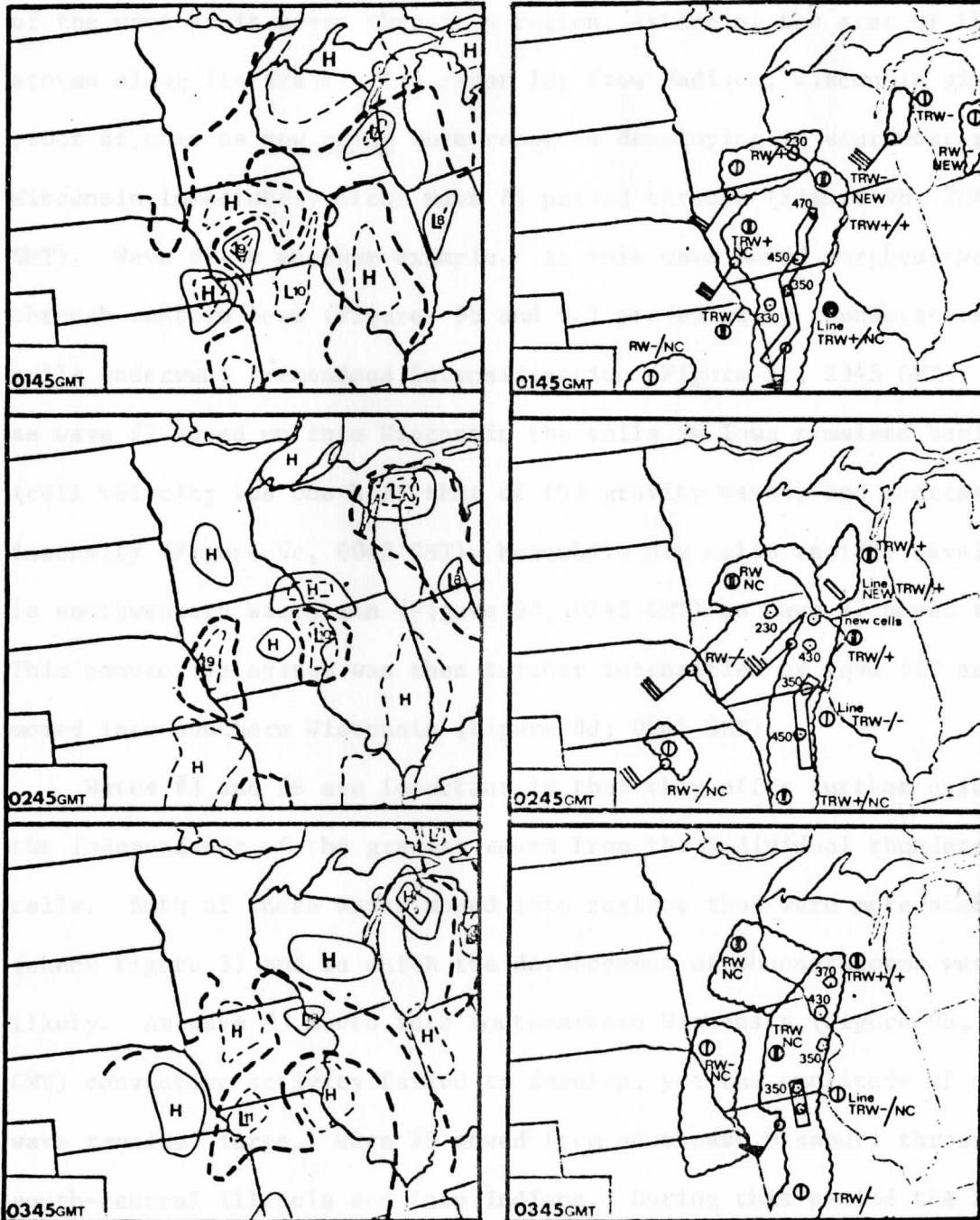


Figure 9d. Pressure perturbation and radar depiction analyses. See Figure 9a for entire legend.

knots while the cell velocity was merely 35 knots. Thus the appearance of the same area of thunderstorms moving with a particular wave is deceptive. Rather, new cells developed slightly behind the trough of the wave as it moved through a region, extending the area of thunderstorms along its track. The radar log from Madison, Wisconsin gives proof of this as new cells were reported developing in southwestern Wisconsin immediately after wave #4 passed through (Figure 9b, 2045 GMT). Wave #7 is another example. As this wave moved northeastward through eastern Iowa (Figures 9b and 9c) pre-existing thunderstorm cells underwent tremendous intensification (Figure 9c, 2345 GMT). Then as wave #7 moved on into Wisconsin the cells in Iowa remained behind (cell velocity was one half that of the gravity waves) and decreased in intensity (Figure 9c, 0045 GMT). Meanwhile new cells rapidly developed in southwestern Wisconsin (Figure 9d, 0145 GMT) as wave #7 moved through. This convective system was then further intensified by wave #10 as it moved into southern Wisconsin (Figure 9d, 0145 GMT).

Waves #3 and #8 are important in that they offer further evidence of the independence of the gravity waves from the individual thunderstorm cells. Both of these waves moved into regions that were more stable (check Figure 3) and in which the development of thunderstorms was less likely. As wave #3 moved into southeastern Wisconsin (Figure 9b, 2045 GMT) convective activity failed to develop, yet the amplitude of the wave remained large. Wave #8 moved from southeast Missouri through south-central Illinois and into Indiana. During this period the St. Louis radar log indicated that no echos were detected along the track of the wave (Figure 9b & 9c, 2145 GMT - 0045 GMT). Therefore the

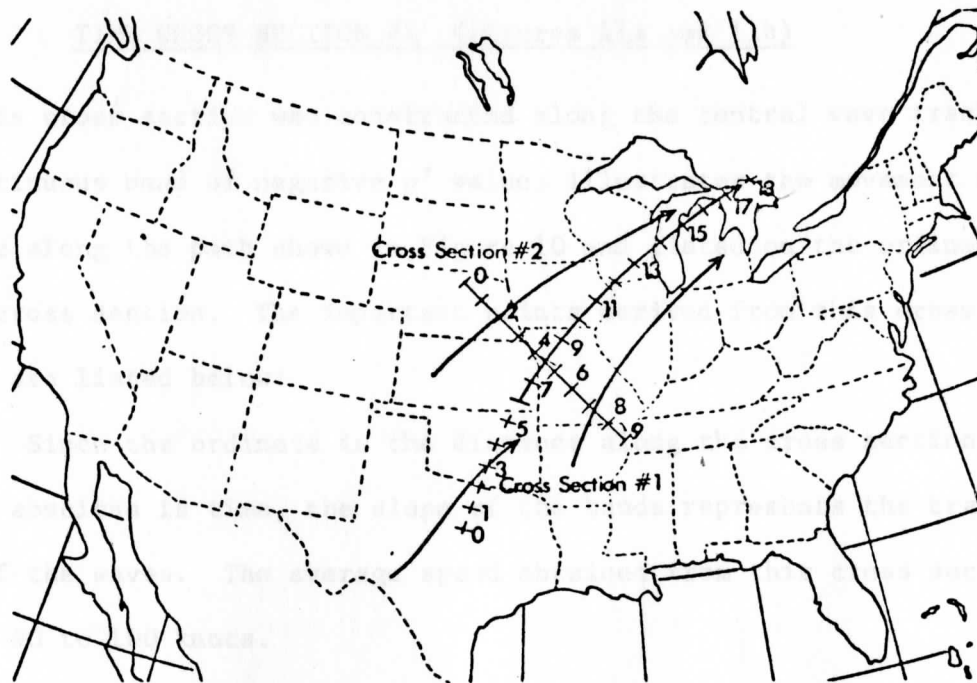


Figure 10. The 4 major tracks of the gravity waves analyzed. Cross Section #1 constructed along central wave track. Cross Section #2 constructed across the wave tracks. The numbers on, or across, the wave tracks indicates position on the cross sections in Figures 11a and 11b.

observed gravity waves were not the result of convective storms, but apparently acted as a forcing function for such storms in this case.

The movement of the gravity waves for the twenty-four hour period (0000 - 2400 CST, May 18, 1971) seemed to be restricted to three major tracks (Figure 10). To summarize the wave movement and the response of the atmosphere to the gravity waves for the entire twenty-four hour period, a time cross section was analyzed across all three tracks as well as one along the central track. The data for these cross sections are the pressure perturbation values taken from the numbered points (Figure 10) every fifteen minutes.

TIME CROSS SECTION #1 (Figures 11a and 11b)

This cross section was constructed along the central wave track. The continuous band of negative p' values illustrates the movement of the wave along the path shown in Figure 10 and listed on the ordinate of the cross section. The important points derived from this cross section are listed below:

1) Since the ordinate is the distance along the cross section and the abscissa is time, the slope of the bands represents the trace speed of the waves. The average speed obtained from this cross section is 90 to 100 knots.

2) There are two sets of waves depicted on this diagram. One set originated in Texas during the morning and moved up to southern Kansas. The late afternoon p' values in Oklahoma and northern Texas were a result of a squall line and are not due to wave activity.

The other set of waves originated in Kansas during the entire twenty-four hour period and moved northeastward toward northern Michigan. It is this set of waves that most of the analysis will be focused upon.

3) The origin of this set of waves appeared to be in east central and northeastern Kansas, near the developing cyclone.

4) The duration of each wave is nearly 10 hours. A 10 hour duration has also been observed for the gravity waves in Japan (Matsumoto and Ninomiya 1967).

5) Moving along the abscissa at point #12 (Iowa) a minimum p' value is attained every 2.5 to 3.0 hours indicating that this area experienced gravity waves with a three hour period.

6) Figure 11b related surface weather reports to gravity waves. A cyclical pattern is apparent here as the precipitation tends to occur immediately after the passage of the trough of the wave. For the most part, maximum rainfall intensity occurs with positive p' values and the rainfall decreases in intensity with the onset of the next wave.

7) Note that in northern Missouri and Iowa (points 8 through 12) the precipitation outburst became less intense as the morning progressed:

- a) Wave passage at 0600 CST (point 10) was followed by significant rainfall.
- b) Wave passage at 0900 CST (point 10) was followed by scattered, very light rain and thundershowers.
- c) Wave passage at 1200 CST (point 10) was noticeably dry in that no precipitation was observed in Missouri and scattered light thundershowers were reported in eastern Iowa.

The important factor here is that the existence and nature of the waves are independent of the intensity of the convective storms. The amplitudes of the waves remained constant during the morning hours. Yet the intensity of the subsequent thunderstorms decreased during this period, indicating perhaps an increase in the stability of the atmosphere. It is apparent therefore that proper conditions must exist if the gravity waves are to initiate convective storms. This point will be covered in section III.

8) Later in the afternoon the waves appeared to initiate storms that were very intense with tornadoes, windstorms, and hail reported throughout Iowa. The tornadoes and windstorms occurred within the negative p' regions. This is consistent with theoretical and diagnostic studies (Eom 1972, Brunk 1949) which show the largest wind velocity to be associated with the trough of the gravity wave.

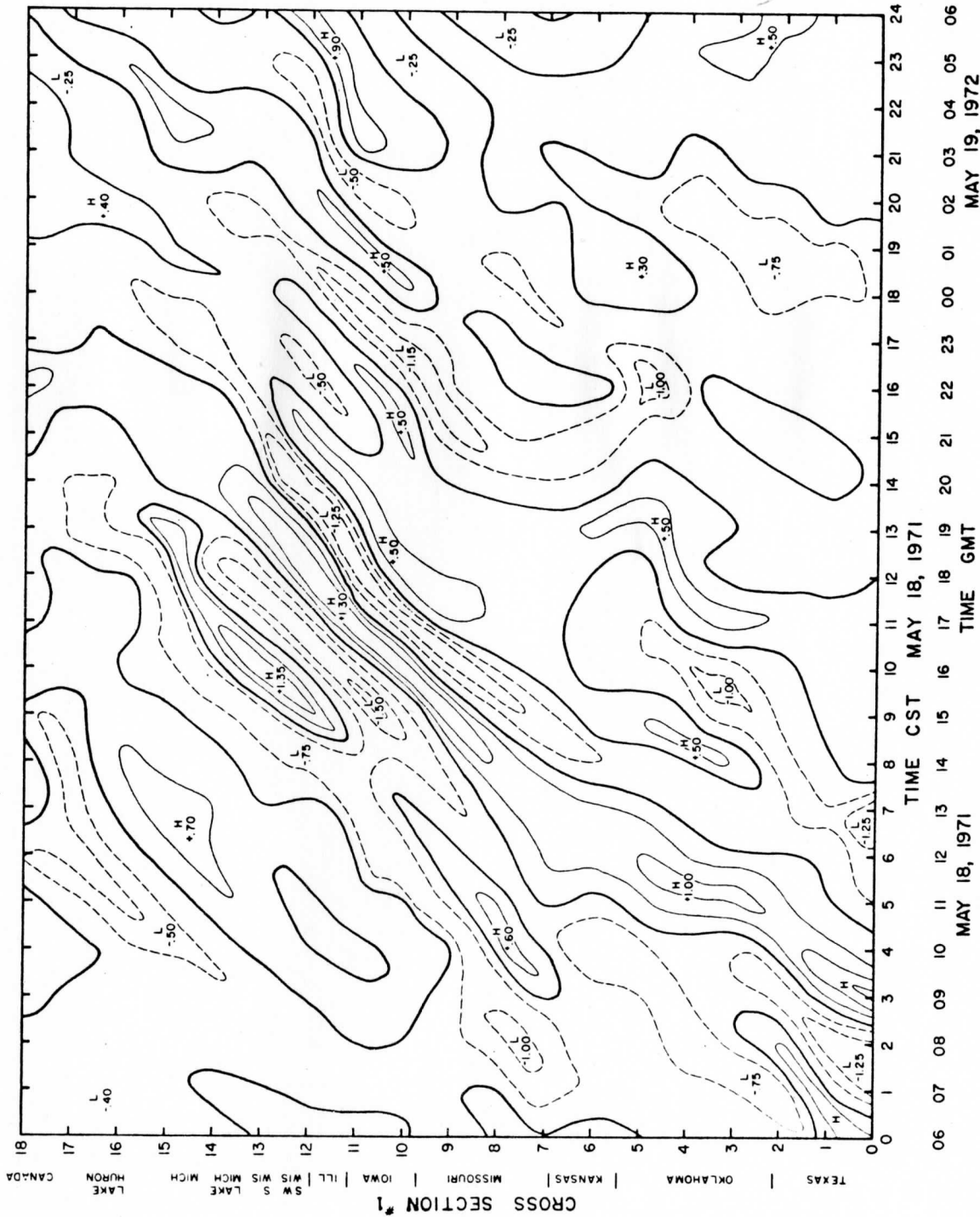


Figure 11a. Time Cross Section #1 of the pressure perturbation values (mb). - - - - negative p',
—— positive p', ——— p' = 0. The cross section is analyzed at intervals of 0.5 mb.

Figure 11b. Time Cross Section #1 with surface weather reports. The shaded area represents $-p'$. Dashed lines represent the tracks of the gravity waves (from Figure 11a).

Legend for surface weather reports:

- thundershower
- rainshower

Intensity

- (--) very light
- (-) light
- () moderate
- (+) heavy

- ⊙ windstorm
- ⊕ tornado

- ⊖ one station reporting precipitation
- ⊗ two or more stations concurrently reporting precipitation

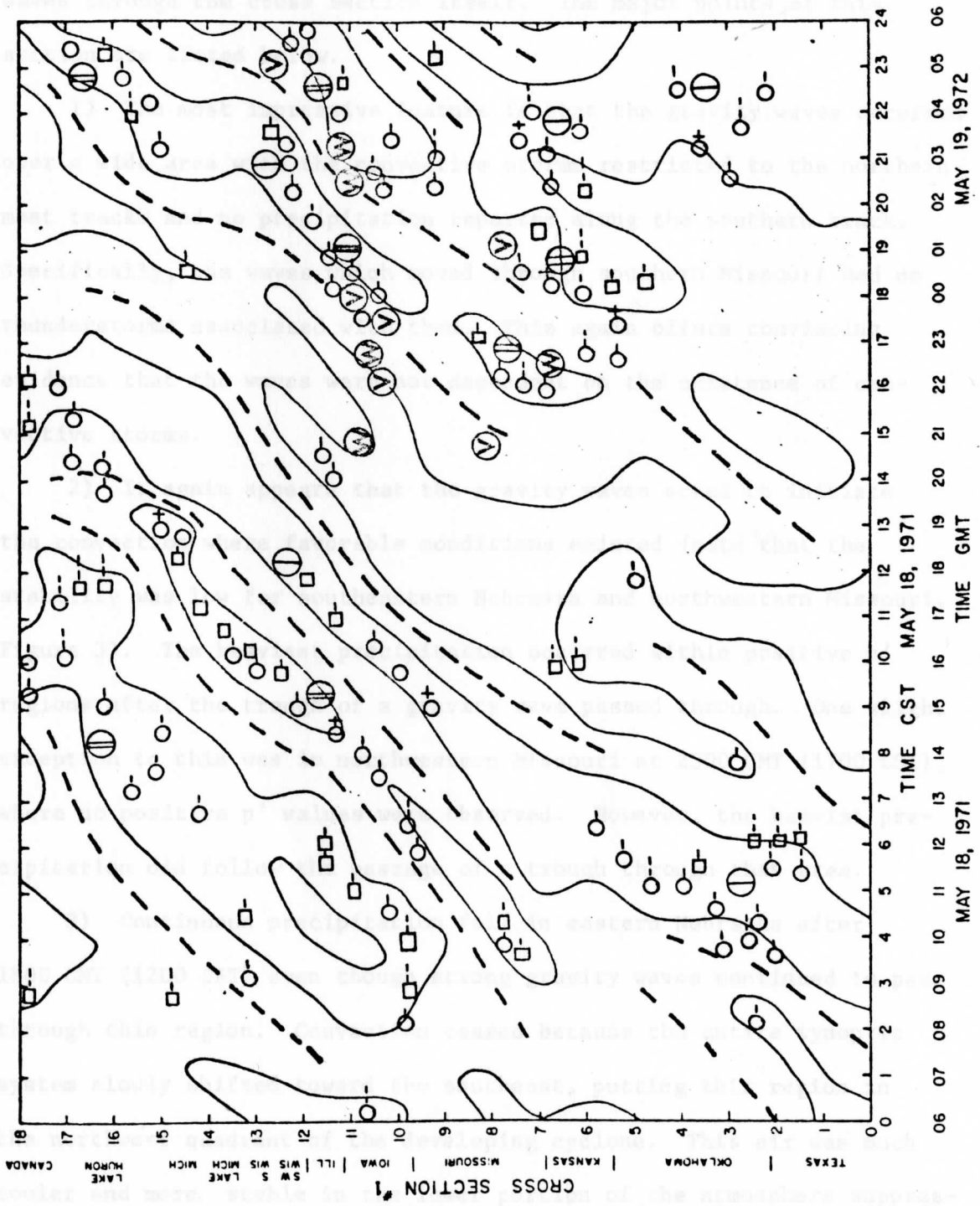


Figure 11b.

TIME CROSS SECTION #2 (Figures 12a and 12b)

This cross section was constructed perpendicular to the three wave tracks (Figure 10) and illustrates the movement of the gravity waves through the cross section itself. The major points of this section are listed below.

1) The most impressive feature is that the gravity waves occurred over a wide area with the convective storms restricted to the northern most tracks and no precipitation reported along the southern track. Specifically, the waves which moved through southern Missouri had no thunderstorms associated with them. This again offers convincing evidence that the waves were not dependent on the existence of convective storms.

2) It again appears that the gravity waves acted to initiate the convection where favorable conditions existed (note that the stability was low for southeastern Nebraska and northwestern Missouri, Figure 3). The heaviest precipitation occurred within positive p' regions after the trough of a gravity wave passed through. One slight exception to this was in northwestern Missouri at 2300 GMT (1700 CST), where no positive p' values were observed. However, the heaviest precipitation did follow the passage of a trough through that area.

3) Continuous precipitation fell in eastern Nebraska after 1800 GMT (1200 CST) even though strong gravity waves continued to pass through this region. Convection ceased because the entire synoptic system slowly shifted toward the southeast, putting this region in the northwest quadrant of the developing cyclone. This air was much cooler and more stable in the lower portion of the atmosphere suppressing any significant convection.

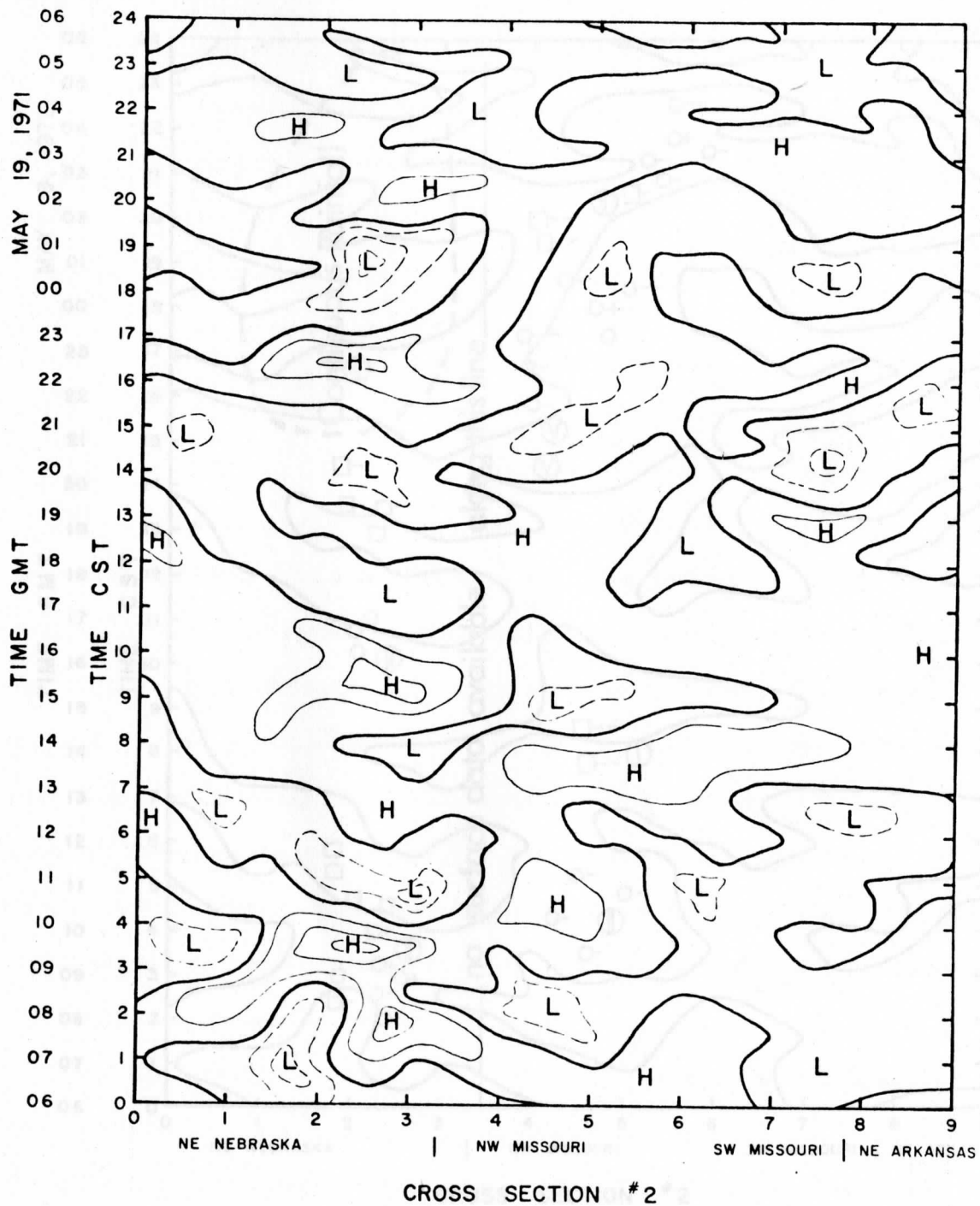


Figure 12a. Time Cross Section #2 of the pressure perturbation values (mb). - - - negative p' , ——— positive p' , ——— $p' = 0$. The cross section is analyzed at intervals of 0.5 mb.

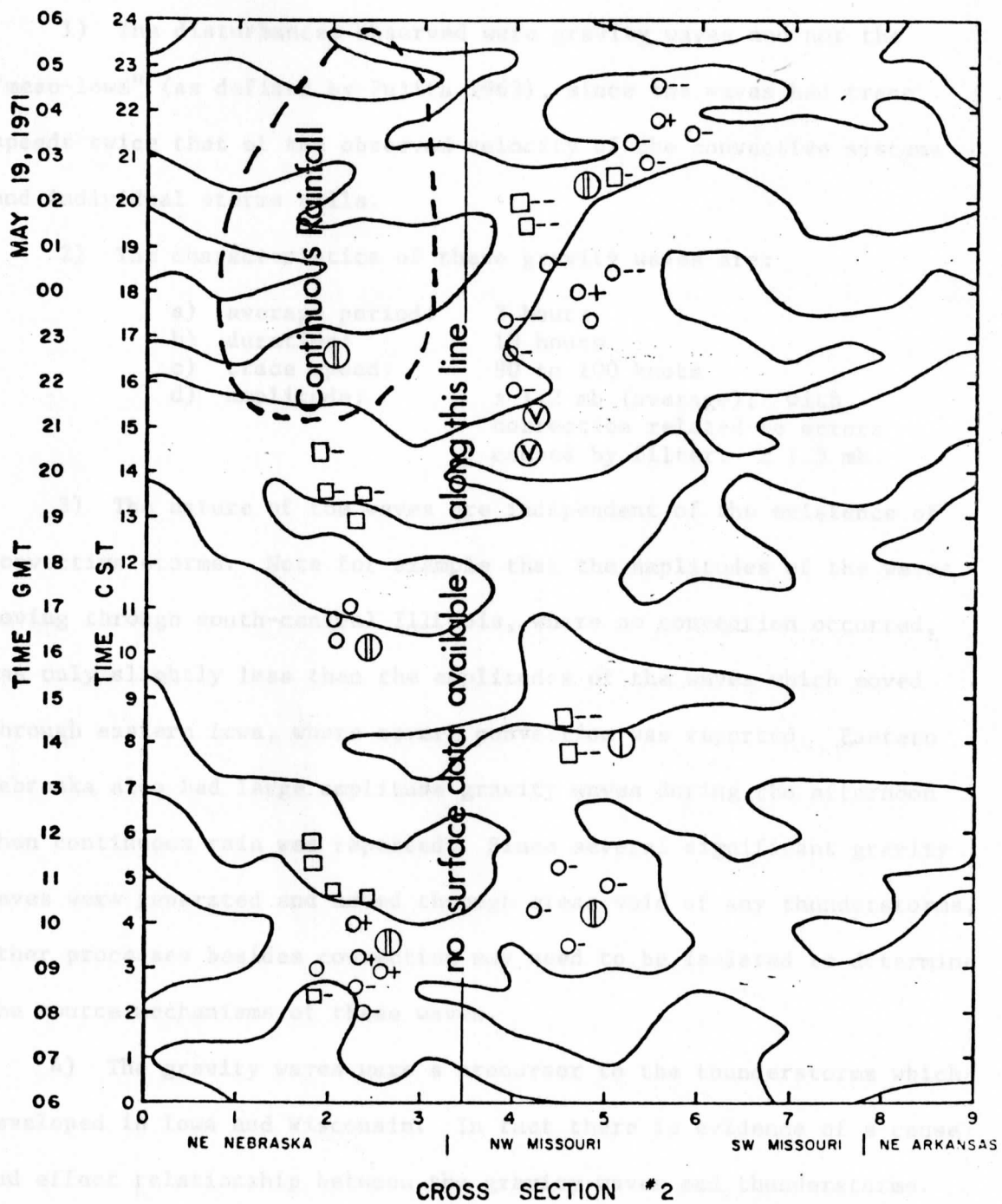


Figure 12b. Time Cross Section #2 with surface weather reports. See Figure 11b for entire legend.

Summary of the Pressure Perturbation Analysis

The four major points derived from this extensive analysis are listed below:

1) The disturbances observed were gravity waves and not the "meso-lows" (as defined by Fujita 1963), since the waves had trace speeds twice that of the observed velocity of the convective systems and individual storms cells.

2) The characteristics of these gravity waves are:

- a) average period: 3 hours
- b) duration: 10 hours
- c) trace speed: 90 to 100 knots
- d) amplitude: ± 1.2 mb (average); with correction related to errors caused by filter: ± 1.5 mb

3) The nature of the waves are independent of the existence of convective storms. Note for example that the amplitudes of the waves moving through south-central Illinois, where no convection occurred, was only slightly less than the amplitudes of the waves which moved through eastern Iowa, where severe convection was reported. Eastern Nebraska also had large amplitude gravity waves during the afternoon when continuous rain was reported. Since several significant gravity waves were generated and moved through areas void of any thunderstorms, other processes besides convection may need to be isolated to determine the source mechanisms of these waves.

4) The gravity waves were a precursor to the thunderstorms which developed in Iowa and Wisconsin. In fact there is evidence of a cause and effect relationship between the gravity waves and thunderstorms. As the gravity waves moved through this area existing convective systems reintensified and new cells rapidly developed extending the area of

thunderstorms along the track of the waves. Section III, which deals with the capability of gravity waves to initiate convective storms, will offer additional evidence that the waves could in fact initiate these storms.

Section II Part 4

A Comparison of the Observations With a Numerical Model of Subsynoptic Scale Gravity Waves

A comparison was made between the observations of this case study and the results of a numerical model of gravity waves derived by Eom (1972). The objective of this comparison is to check the apparent time lag between the passage of the trough of the wave and the onset of the precipitation, which appears to be associated with the ridge.

The incompressible, homogeneous, three layer model derived by Eom (1972) has the assumptions: linear, adiabatic, hydrostatic, inviscid, and no mean motion in the lowest layer. Therefore the atmosphere is divided into three levels. The lowest level has no mean motion, constant density, and a mean depth H_1 , with the middle level having a constant horizontal mean motion. The third level is a passive stable layer which is preferable to the rigid top or free surface boundary conditions. In short, this model describes the behavior of internal tropospheric gravity waves within a simplified, sheared environment. The model proved to be successful in Eom's case study as the values obtained from the eigenfunctions describing the trace speed and horizontal wind perturbations due to the gravity waves were in very close agreement with the surface observations (Eom 1972).

The model seemed especially applicable to this case study since the weather situation was very similar to that studied by Eom. Both cases consisted of a period of cyclogenesis, significant jet streaks, and similar upper air soundings with:

- 1) a nearly isothermal layer in the bottom portion of the sounding, topped by a lapse rate which is nearly constant and,
- 2) inversion layers providing an interface for the propagation of the waves.

Given the simple wave form $e^{ik(x-ct)}$, the surface pressure is given at $t = 0$ as:

$$p_s(x) = \text{Re} \{p' e^{ikx}\}$$

p' is the amplitude of the pressure perturbation at the surface

k is the wave number in the direction of propagation

Assuming p' is real positive

$$p_s(x) = p' \cos(kx) \quad (1)$$

The vertical motion within the first layer at $t = 0$ is simply:

$$w_1(x,z) = \text{Re} \{w_1'(z) e^{ikx}\} \quad (2)$$

$w_1'(z)$ at $z = H_1$ was derived by Eom (1972) and is given as:

$$w_1' = -iMp' \quad (3)$$

where $M = \frac{kH_1}{c\rho_0}$ = real positive if c is positive

w_1' is $w_1'(z)$ at $z = H_1$

c trace speed along x axis

ρ_0 surface density

H_1 mean depth of the first layer

i $\sqrt{-1}$

The profile of the vertical motion may also be determined within the layer $z = 0$ to $z = H_1$. Given the boundary conditions: w_1' (surface) = 0 and $w_1'(z = H_1) = W_1'$:

$$w_1'(z) = \frac{z}{H_1} W_1' \quad (\text{for } z \text{ less than } 3 \text{ km}) \quad (4)$$

Note that the equation is consistent with the boundary conditions and also that the linear profile is consistent with the model assumption of (vertically) constant horizontal motion within the layer.

It follows from equation (2) that

$$w_1(x_1, z) = \frac{z}{H_1} M p' \cos(kx - \pi/2) \quad (5)$$

It is immediately obvious that the vertical motion is 90° out of phase with the pressure oscillation. Therefore if \underline{c} (trace speed) is positive, the maximum rising motion at H_1 will be found between the trough and the advancing ridge of the wave (Figure 13).

The vertical motion $w_1(z)$ may also be defined in terms of the parcel displacement D_1 as:

$$w_1(x, z, t) = \frac{dD_1}{dt} = \frac{\partial D_1}{\partial t} + U_1 \frac{\partial D_1}{\partial x}$$

where U_1 is the mean horizontal wind speed. Since U_1 was assumed = 0,

$$\frac{\partial D_1}{\partial t} = w_1(x, z, t) \quad (6)$$

D_1 can also be represented by the simple wave form:

$$D_1 = \text{Re} \{ D_1' e^{ik(x-ct)} \}$$

Substituting this and the equivalent form of equation (5) (for w_1') and inserting these variables into equation (6) yields:

$$\frac{\partial \text{Re} \{D_1' e^{ik(x-ct)}\}}{\partial t} = \frac{z}{H_1} \text{Re} \{-iMp' e^{ik(x-ct)}\}$$

If follows

$$D_1' = \frac{z}{H_1} \frac{M}{kc} p' \quad (7)$$

Therefore by setting $t = 0$

$$D_1(x, z) = \frac{z}{H_1} \frac{M}{kc} p' \cos(kx) \quad (8)$$

Since M is positive and c (trace speed) is assumed to be positive, the displacement of the parcel is in phase with the surface pressure perturbation. Therefore maximum displacement occurs at the ridge of the wave (Figure 13).

Thus according to this model the maximum rising motion should occur midway between the trough and the advancing ridge with maximum displacement of the parcels occurring at the ridge of the wave. If the atmosphere is conducive to convective storms, the development phase (as defined by Byers and Braham, 1949) should occur sometime during the period of upward vertical motion. Maximum convective activity should coincide with the period of maximum parcel displacement (at the ridge of the wave).

The observations fit this model very well as significant precipitation occurred after the trough passage with maximum rainfall usually found near the time of passage of the ridge. Note that the time between the ridge line and trough line is 90 minutes which is enough time for severe thunderstorm cells to go through the development and mature precipitating phases (Byers and Braham 1949, Schlesinger 1972).

Figure 13. Profiles of surface pressure (left), vertical motion (right) and parcel displacement (top) of a convective wave. The model is based on the model of Byers and Braham (1949). Trace speed is assumed to be the UGT.

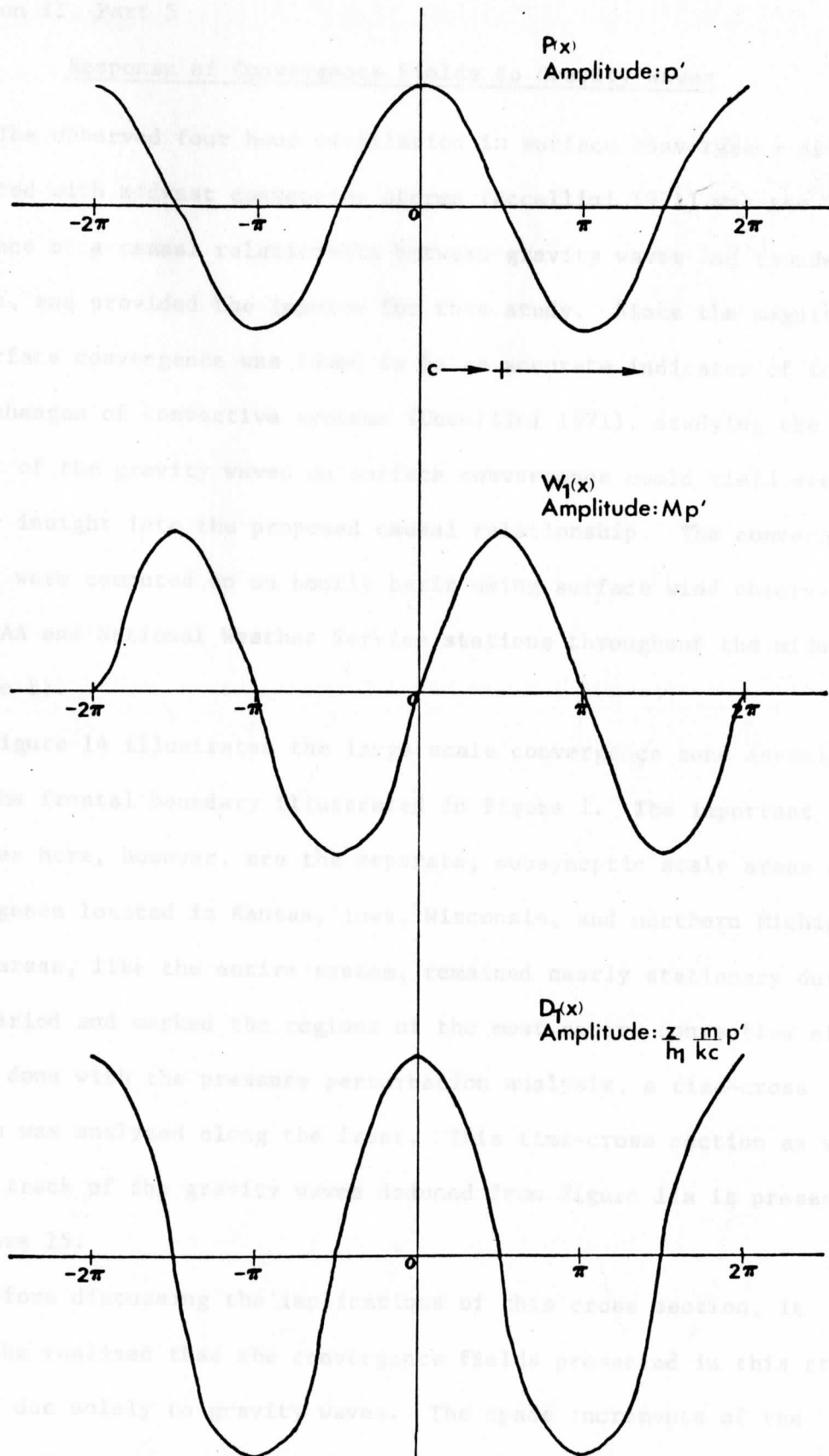


Figure 13. Profiles of surface pressure $P(x)$, vertical motion $w_1(x)$, and parcel displacement $D_1(x)$, determined through numerical model derived by Eom (1972). Trace speed c is positive to the right.

Section II Part 5

Response of Convergence Fields to Gravity Waves

The observed four hour oscillation in surface convergence associated with midwest convective storms (Uccellini 1971) was the initial evidence of a causal relationship between gravity waves and thunderstorms, and provided the impetus for this study. Since the magnitude of surface convergence was found to be an accurate indicator of intensity changes of convective systems (Uccellini 1971), studying the effect of the gravity waves on surface convergence could yield even deeper insight into the proposed causal relationship. The convergence values were computed on an hourly basis using surface wind observations from FAA and National Weather Service stations throughout the midwest (Figure 8).

Figure 14 illustrates the large scale convergence zone associated with the frontal boundary illustrated in Figure 1. The important features here, however, are the separate, subsynoptic scale areas of convergence located in Kansas, Iowa, Wisconsin, and northern Michigan. These areas, like the entire system, remained nearly stationary during this period and marked the regions of the most severe convective storms. As was done with the pressure perturbation analysis, a time-cross section was analyzed along the front. This time-cross section as well as the track of the gravity waves deduced from Figure 11a is presented in Figure 15.

Before discussing the implications of this cross section, it should be realized that the convergence fields presented in this study are not due solely to gravity waves. The space increments of the

reporting stations (Figure 8) do not allow for a computation of the mesoscale values needed to isolate this particular aspect of the waves as was done in Matsumoto and Ninomiya (1967). Rather, these convergence fields reflect the influence of larger scale features. The entire frontal zone, as illustrated in Figure 14 is very similar to the model presented by Gall (1972). Gall and Cahir (1971) have shown that the frontal convergence zones are influenced by the adjustment process near the jet core. This appears to be the case here, as strong jet cores were prevalent over the frontal boundary (Figure 2), along which the time-cross section in Figure 15 was constructed.

The important features of the convergence time-cross section are listed below:

- 1) The four areas of maximum convergence are each identified, being located in northeastern Kansas (C1), northeastern Iowa (C2), east-central Wisconsin (C3), and northern Michigan (C4).
- 2) The lack of slope indicated that these fields were not transient, reflecting the stationarity of the entire system. To further substantiate this contention, the twenty-four hour rainfall map for May 18, 1971 is presented in Figure 16. Even though rainfall occurred along the entire front, the heaviest amount fell in regions of the strongest convergence. It is believed therefore that the stationary nature, reflected by the convergence fields, is real and not a result of numerical aspects or an inhomogeneous station density.
- 3) The four convergence zones pulsed in intensity with periods of two to five hours.
- 4) Included on the cross section are the tracks of the gravity waves (heavy dashed lines) derived from the pressure perturbation

cross section #1 (Figure 11a). This analysis indicates that for the most part, an increase in the magnitude of the surface convergence coincided with the passage of a gravity wave.

A picture of the interaction between gravity waves and an environment, primed for convective storms by the synoptic circulation, can now be drawn. Figure 17 illustrates the pressure, convergence, precipitation rates and severe weather reports for east-central Iowa. This figure indicates that after the passage of a trough of a wave, or nearly at the time of the ridge, there was a peak in the magnitude of the surface convergence and rainfall rates (except at 1800 CST). The intensity of the storms, as indicated by surface reports, also increased after the passage of the trough. As the waves pass on, the magnitudes of convergence, rainfall rates, and storm intensity all decreased, tending toward a minimum value with the onset of the next wave.

A time lag between the passage of the wave trough and convergence maximum should be expected (check vertical motion profile in Section II part 4) while the rainfall maximum should coincide with the ridge of the wave (Section II Part 4). But the instantaneous reaction of the convergence field and rainfall rates could not be measured here because this data was available on an hourly basis only. The important feature however is that the maximum values did occur shortly after the passage of the trough of the gravity wave, and that a cyclical pattern (with a two to four hour period) is quite apparent. This response of the atmosphere to the gravity wave favorably agree with the results obtained from the numerical model (Section II Part 4), and reflects an ability of these waves to generate thunderstorms. Additional evidence of this proposed relationship is offered in the following section.

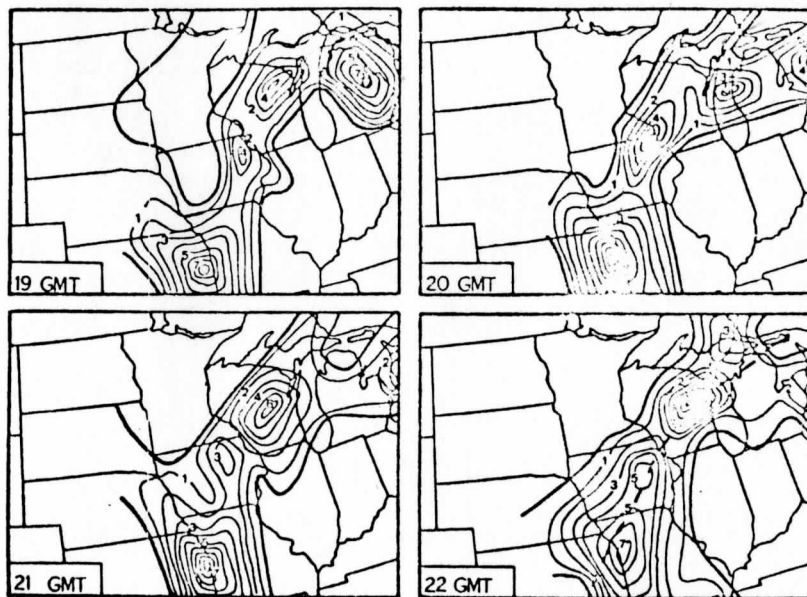


Figure 14. Surface convergence ($\times 10^{-5} \text{ sec}^{-1}$) for the time period 1900 through 2200 GMT, May 18, 1971. Heavier line in the analysis is the line of zero convergence with the interval in the analysis equal to $1 \times 10^{-5} \text{ sec}^{-1}$. The dashed line in the 2200 GMT panel indicates the line along which the convergence time cross section was constructed.

Figure 15. Surface convergence time cross section with tracks of the gravity waves - - - - - (taken from Figure 11a). The shaded area represents maximum convergence ($|\text{convergence}| > 4.0 \times 10^{-5} \text{ sec}^{-1}$). The center line of unshaded area is: convergence = $2.0 \times 10^{-5} \text{ sec}^{-1}$ and represents smallest magnitude of convergence analyzed on this cross section.

Figure 16. Total rainfall for the 24 hour period: 0000 CST through 2400 CST, May 18, 1971. Rainfall data obtained from the statewide Hourly Precipitation Data (published by the U. S. Dept. of Commerce). The interval is 0.5 inches.

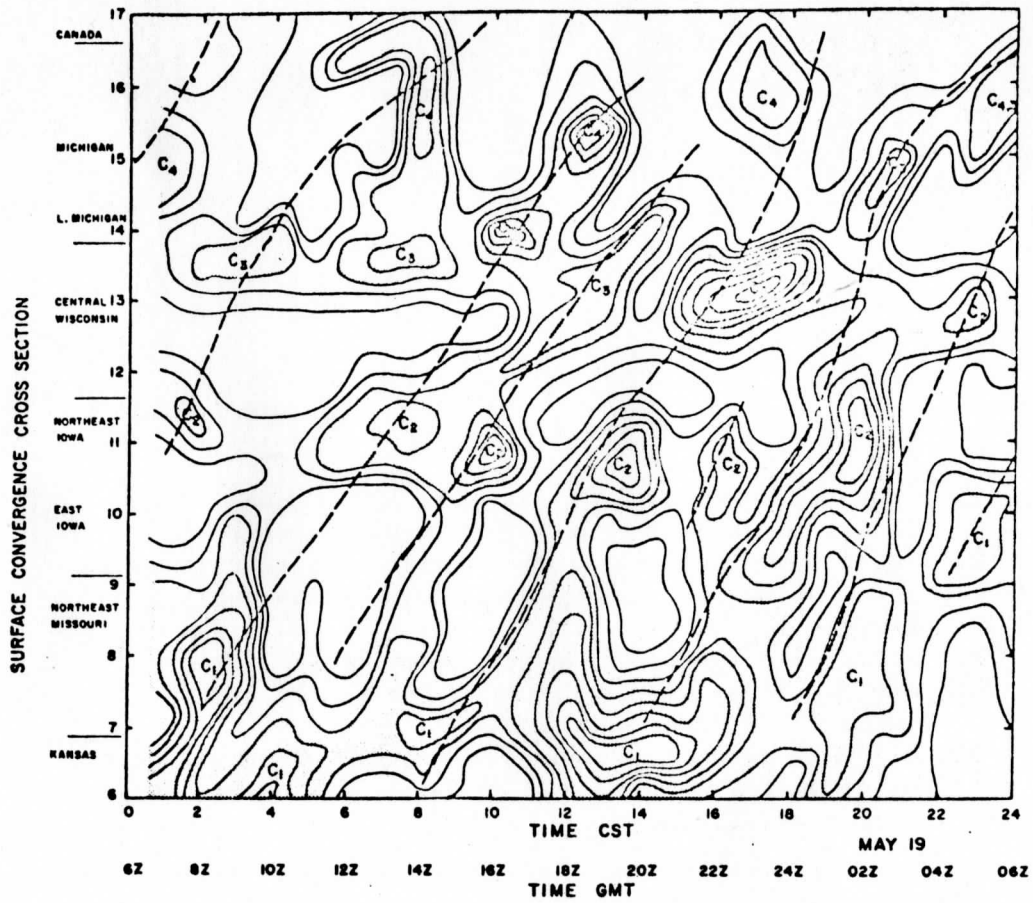


Figure 15.

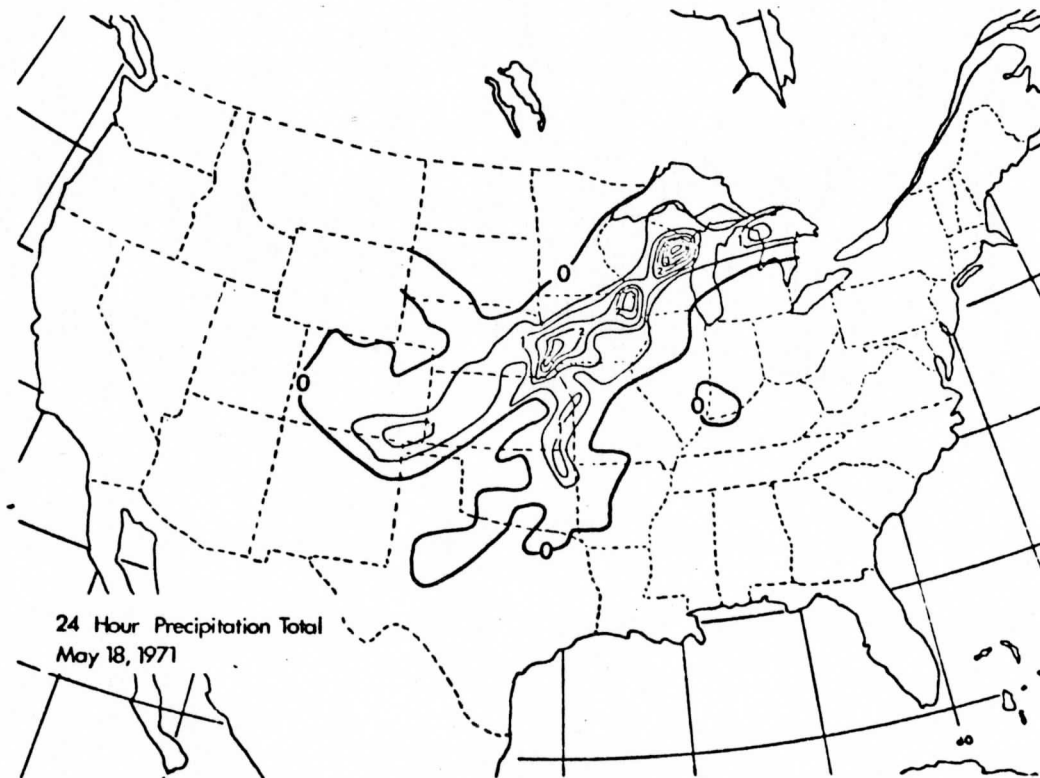


Figure 16.

- Figure 17.
- 1) Pressure perturbation trace for east-central Iowa (point 11 on time cross section #1 Figure 11a).
 - 2) Surface convergence ($\times 10^{-5} \text{ sec}^{-1}$) for east-central Iowa (point 11 on convergence time cross section Figure 15).
 - 3) Storm data (surface weather reports) for east-central Iowa. Check Figure 4 for entire legend, (note W indicates wind storm).
 - 4) Rainfall rates (from statewide Hourly Precipitation Data, published by the U. S. Dept. of Commerce) for east-central Iowa).

The vertical dashed lines indicate the trough line of the gravity waves.

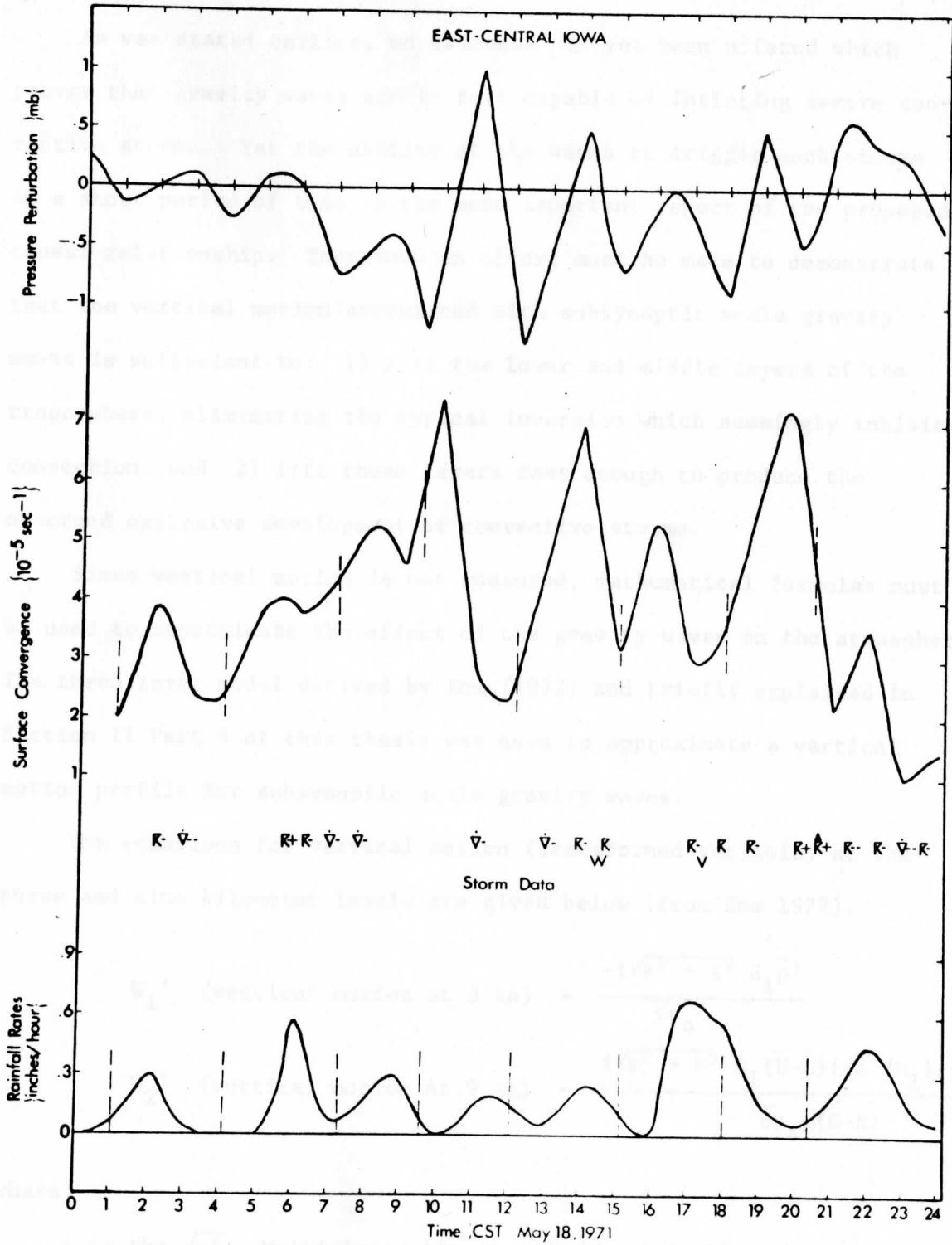


Figure 17.

Section III

The Ability of Gravity Waves to Initiate Severe Convective Storms

As was stated earlier, no evidence has yet been offered which proves that gravity waves are in fact capable of initiating severe convective storms. Yet the ability of the waves to trigger such storms in a short period of time is the most important aspect of the proposed causal relationship. Therefore an effort must be made to demonstrate that the vertical motion associated with subsynoptic scale gravity waves is sufficient to: 1) lift the lower and middle layers of the troposphere, eliminating the typical inversion which seemingly inhibit convection, and 2) lift these layers fast enough to produce the observed explosive development of convective storms.

Since vertical motion is not measured, mathematical formulas must be used to approximate the effect of the gravity waves on the atmosphere. The three layer model derived by Eom (1972) and briefly explained in Section II Part 4 of this thesis was used to approximate a vertical motion profile for subsynoptic scale gravity waves.

The equations for vertical motion (transformed variable) at the three and nine kilometer levels are given below (from Eom 1972).

$$W_1' \text{ (vertical motion at 3 km)} = \frac{-i\sqrt{k^2 + \ell^2} H_1 \bar{p}'}{\bar{c}\rho_0}$$

$$W_2' \text{ (vertical motion at 9 km)} = \frac{i\sqrt{k^2 + \ell^2} H_1 (\bar{U}-c) [(\bar{c}/H_1) - g(1-N)] \bar{p}'}{\bar{c}\rho_0 g(G-N)}$$

where:

i is the $\sqrt{-1}$. Multiplying the equation by i implies that the vertical velocity would have a 90° phase shift with respect to the pressure perturbation (see Section II part 4).

- H_1 depth of the first layer = 3km = 3.0×10^5 cm
- ρ_0 air density at earth's surface ($T = 10^\circ\text{C}$, $P = 1000$ mb)
 $\rho_0 = 1.2 \times 10^{-3}$ g/cm³
- \bar{c} an average trace speed of the gravity waves observed in this case study = 4.5×10^3 cm/sec
- k wave number along axis of movement = $[2\pi/(\text{wavelength along axis})]$
 $= 2\pi/3.0 \times 10^5 \text{ m} = (2\pi) (3.0 \times 10^7)^{-1} \text{ cm}^{-1}$
- l wave number across axis of movement = $[2\pi/(\text{wavelength across axis})]$ = $2\pi/2.2 \times 10^5 \text{ m} = (2\pi) (2.2 \times 10^7)^{-1} \text{ cm}^{-1}$
- U average wind speed in the upper layer = 20 m/sec = 2.0×10^3 cm/sec
- g gravity = 980 cm/sec²
- N $\rho_3/\rho_1 = .78$
- G $\rho_2/\rho_1 = .90$
- p' an average amplitude of the gravity waves observed in this case study - 1.5 mb

Using these equations the maximum vertical motions were found to be:

$$W_1'(z = 3 \text{ km}) = 30 \text{ cm/sec}$$

$$W_2'(Z = 9 \text{ km}) = -6 \text{ cm/sec}$$

After assuming that $w(0)$ (vertical motion at surface) is zero, a linear profile was constructed from $z=0$ to $z=3\text{km}$ to $z=9\text{km}$ which is representative of the vertical motion midway between the trough and the advancing ridge of the wave (Figure 18). As a check of the values obtained, note that the 30 cm/sec value at three kilometers would correspond to a surface convergence value of $1.0 \times 10^{-4} \text{ sec}^{-1}$. This value is equal to that observed for gravity waves in western Japan (Matsumoto and Ninomiya 1967).

To determine the effect of the gravity waves on the atmosphere the "layer lift" procedure was applied to atmospheric soundings. First, the mean vertical velocity $\overline{W}(z)$ was determined for nine sub-layers, each one kilometer deep. Then using the development below, the maximum displacement each of these layers would experience was determined.

From equation 8 (part 4 of Section II) the amplitude of parcel displacement was found to be:

$$D_{1m}(z) = \frac{z}{H_1} \frac{M}{kc} p'$$

The maximum displacement range is simply twice this amplitude:

$$2D_{1m}(z) = 2 \frac{z}{H_1} \frac{M}{kc} p'$$

The product $kc = \text{frequency} = \frac{2\pi}{\tau}$ where τ is simply the period of the wave. Therefore:

$$2D_{1m}(z) = \frac{z}{H_1} M p' \frac{\tau}{\pi}$$

It follows from equation (5) (part 4 of Section II) and the definition of the vertical motion amplitude $w_{1m}(z)$ that

$$2D_{1m}(z) = W_{1m}(z) \frac{\tau}{\pi} \quad (9)$$

The lifting process was further simplified by applying the displacement, formula (9), to the nine sub-layers in the model layers 1 and 2 such that the maximum displacement range for each level is simply

$$2D_{1m}(z) = \overline{W_{1m}(z)} \frac{\tau}{\pi}$$

where the $\overline{\quad}$ indicates an average over the (1 km) sub-layers. The values for $2D_{1m}(z)$ are presented in Figure 18.

Three soundings were selected to test the effect of these gravity waves. Green Bay, Wisconsin (0000 GMT, May 19) and Topeka, Kansas (1200 GMT, May 18) were within the area of significant convective activity while Salem, Illinois (1200 GMT, May 18) was outside the region of convective storms but within the area which experienced gravity waves.

Two factors must be considered to determine the effects of the waves. First, there is the destabilization of the sounding due to the deep extent of the rising motion. This destabilization could be further enhanced by the distribution of moisture usually found in convectively unstable air; that is, dry air over very moist air with the boundary between the two air masses being very sharp. Note that the upper portion of the atmosphere would be cooled dry adiabatically with the lower levels cooled moist adiabatically if saturated, therefore steepening the lapse rate of the environment.

Secondly, the lifting of the layers could sufficiently cool the air for it to become saturated. This was usually the case since the lifting process conserves the mixing ratio allowing moist air to be lifted to higher and cooler levels. Thus if the lapse rate of the sounding is increased beyond the moist adiabatic lapse rate any disturbance (e.g. thermal anomaly, turbulence, smaller scale gravity waves) could force the saturated parcels beyond their level of free convection. These parcels would then accelerate upward and enhance the development of the convective storms.

The change in the sounding was quantified by considering the change in the buoyancy force due to the layer lift procedure. The buoyancy force per unit mass is defined as:

$$g \frac{(T' - T)}{T}$$

where: T' = temperature of parcel

T = temperature of the environment

Now:

$$W_k = \int_{z_1}^{z_2} g \left(\frac{T' - T}{T} \right) dz \quad \text{units: ergs/gm}$$

represents the net work done on a parcel displaced from z_1 to z_2 .

Using the hydrostatic equation and the equation of state:

$$\frac{\partial p}{\partial z} = -\rho g$$

$$P = \rho RT$$

$$W_k = - \int_{P_1}^{P_2} g \left(\frac{T' - T}{T} \right) \frac{RT}{pg} dp$$

$$W_k = - \int_{P_1}^{P_2} T' Rd \ln p + \int_{P_1}^{P_2} TR d \ln p$$

Positive W_k indicates that a parcel would gain kinetic energy from the environment and experience unimpeded vertical motion. Negative W_k indicates that the buoyancy force is working against the vertical movement of the parcel, therefore inhibiting rising motion. W_k was determined for two layers, 850 mb to 700 mb and 850 mb to 500 mb, before and after the wave passed through, to test for significant destabilization due solely to gravity waves.

It was also determined if any levels existed in which parcels would be at their level of free convection after the sounding was destabilized by the layer lift procedure. This would occur for saturated

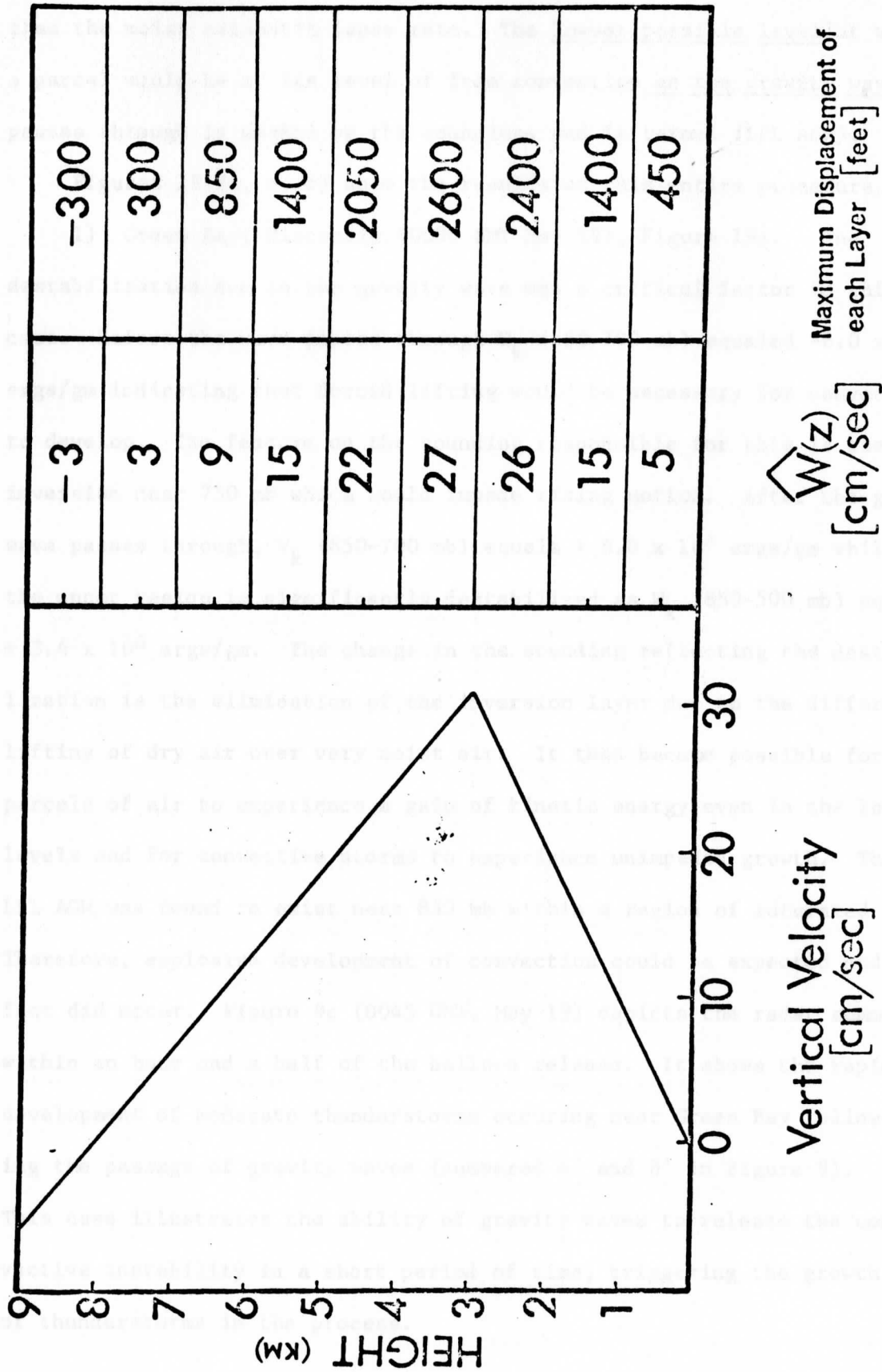


Figure 18. Vertical motion profile, mean vertical motion for each layer, and maximum displacement range for each layer, determined through numerical model derived by Eom 1972 (see text).

parcels situated within an environment having a lapse rate greater than the moist adiabatic lapse rate. The lowest possible level at which a parcel would be at its level of free convection as the gravity wave passes through is marked on the soundings and is termed (LPL AGW).

Figures 19 (a, b, c) show the results of this entire procedure.

1) Green Bay, Wisconsin (0000 GMT May 19), Figure 19a. The destabilization due to the gravity wave was a critical factor in this case. Before the wave passed through W_k (850-700 mb) equaled -6.0×10^5 ergs/gm indicating that forced lifting would be necessary for convection to develop. The feature on the sounding responsible for this is the inversion near 750 mb which would impede rising motion. After the gravity wave passes through, W_k (850-700 mb) equals $+ 8.0 \times 10^5$ ergs/gm while the upper region is significantly destabilized as W_k (850-500 mb) equals $+ 3.4 \times 10^6$ ergs/gm. The change in the sounding reflecting the destabilization is the elimination of the inversion layer due to the differential lifting of dry air over very moist air. It then became possible for parcels of air to experience a gain of kinetic energy even in the low levels and for convective storms to experience unimpeded growth. The LPL AGW was found to exist near 830 mb within a region of saturated air. Therefore, explosive development of convection could be expected and in fact did occur. Figure 9c (0045 GMT, May 19) depicts the radar summary within an hour and a half of the balloon release. It shows the rapid development of moderate thunderstorms occurring near Green Bay following the passage of gravity waves (numbered 4' and 8' in Figure 9). This case illustrates the ability of gravity waves to release the convective instability in a short period of time, triggering the growth of thunderstorms in the process.

2) Topeka, Kansas (1200 GMT, May 18), Figure 19b. The change induced in this sounding appears to be small when considering only W_k . The 850-700 mb layer changed from -1.0×10^5 ergs/gm to 0 ergs/gm indicating that a neutral condition would exist up to 700 mb after the gravity wave passed through. But note that a strong inversion was lifted and weakened considerably (Figure 19b) with a deep super-adiabatic layer appearing on the new sounding. This yielded a large change in W_k (850-500 mb), and since the LPL AGW was again situated in a deep saturated layer, convective storms could be expected. During the morning of the 18th of May, numerous severe thunderstorms developed in northeastern Kansas and southeastern Nebraska as gravity waves passed through (Figure 12b). Again, where conditions favored the development of convection, subsynoptic scale gravity waves were capable of initiating such storms.

3) Salem, Illinois (1200 GMT, May 18), Figure 19c. This sounding was included to demonstrate the fact that gravity waves can initiate convective activity only if the proper conditions exist. Figure 19c indicates that initial conditions were not suitable for convective storms at Salem. The moisture was restricted to a shallow layer near the surface. This layer was capped by a very strong inversion further reducing the possibility of thunderstorms. W_k remained negative and in fact became more negative for both layers after the wave passed through. This was due in large part to the lifting of the inversion level from below the 850 mb level to within the bottom layer (850-700 mb). Since the entire lifting process occurred dry adiabatically the inversion itself was not weakened significantly. No LPL AGW could be found for this sounding. Therefore no convection could develop even

though significant gravity waves moved through this area (Figure 9b, 9c, 12b).

This study illustrates the ability of gravity waves to initiate thunderstorms in areas having the necessary amount and proper distribution of moisture needed for widespread convective activity. The subsynoptic scale waves not only destabilized soundings by eliminating the typical inversions which preclude thunderstorms (Newton 1963), but also could bring parcels of saturated air to their level of free convection. The entire process occurs within one and half hours and could lead to the explosive development, or the reintensification, of thunderstorm cells. This proof of capability and the heretofore observed causal relationship indicate that gravity waves can, and apparently do, initiate the development of severe convective storms.

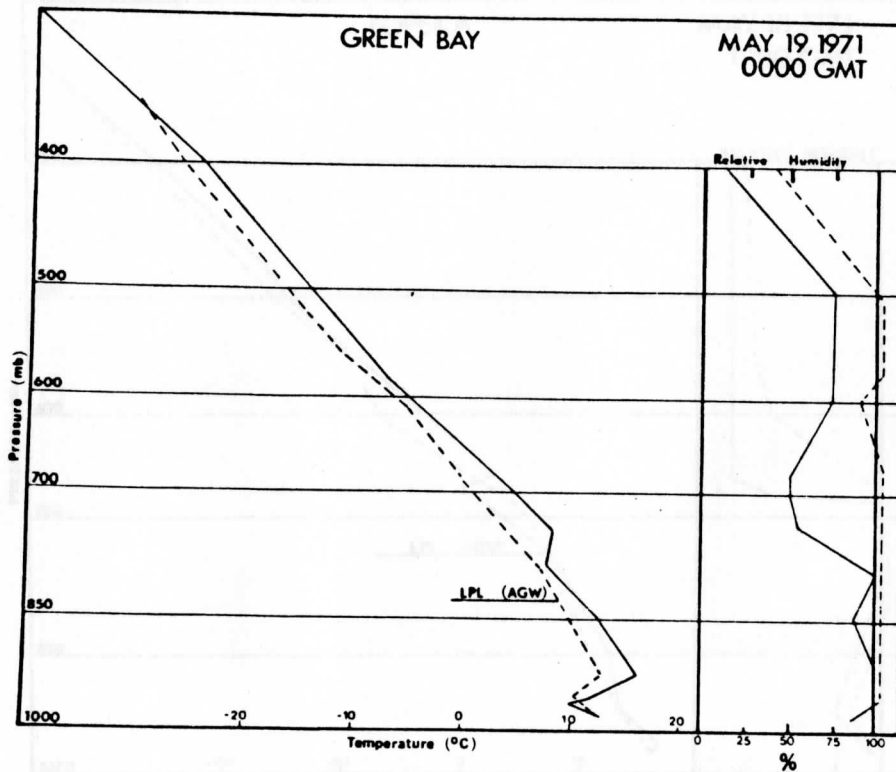
Figure 19a. Atmospheric soundings for Green Bay, Wisconsin 0000 GMT
May 19, 1971

original sounding _____
hypothetical sounding following maximum displacement due
to the gravity wave (see text) - - - - - .

Relative Humidity

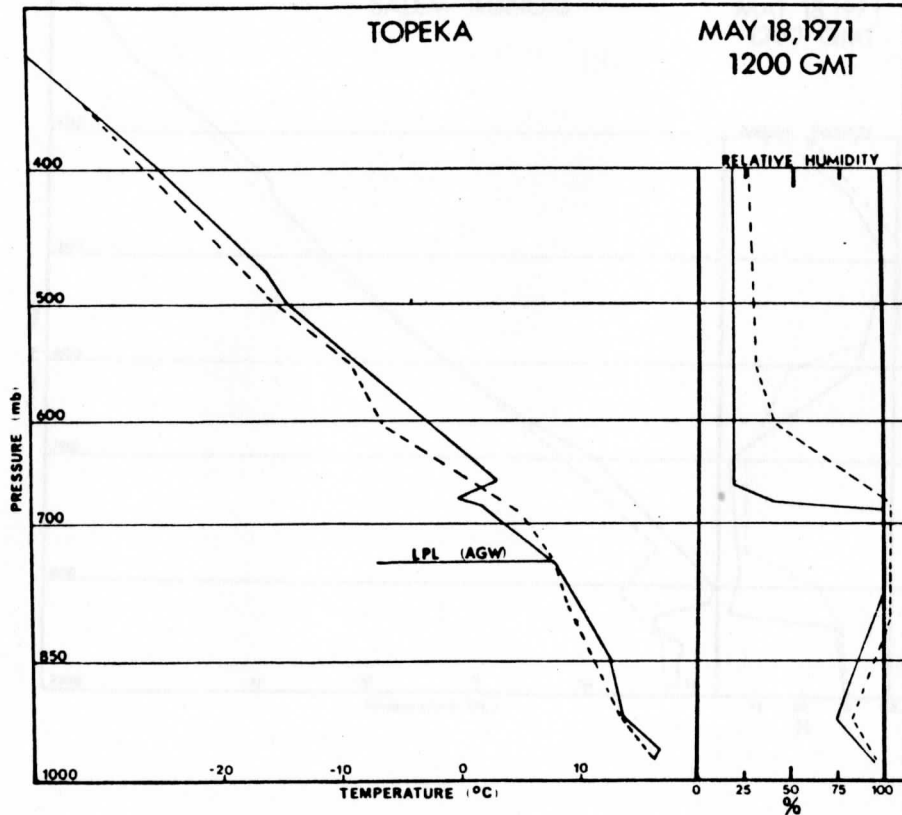
original sounding _____
hypothetical sounding - - -, dashed line beyond 100% re-
presents levels at which liquid water is realized.

LPL (AGW) lowest level at which parcels are brought to
their level of free convection as a result of the
maximum displacement due to the gravity waves (see text).



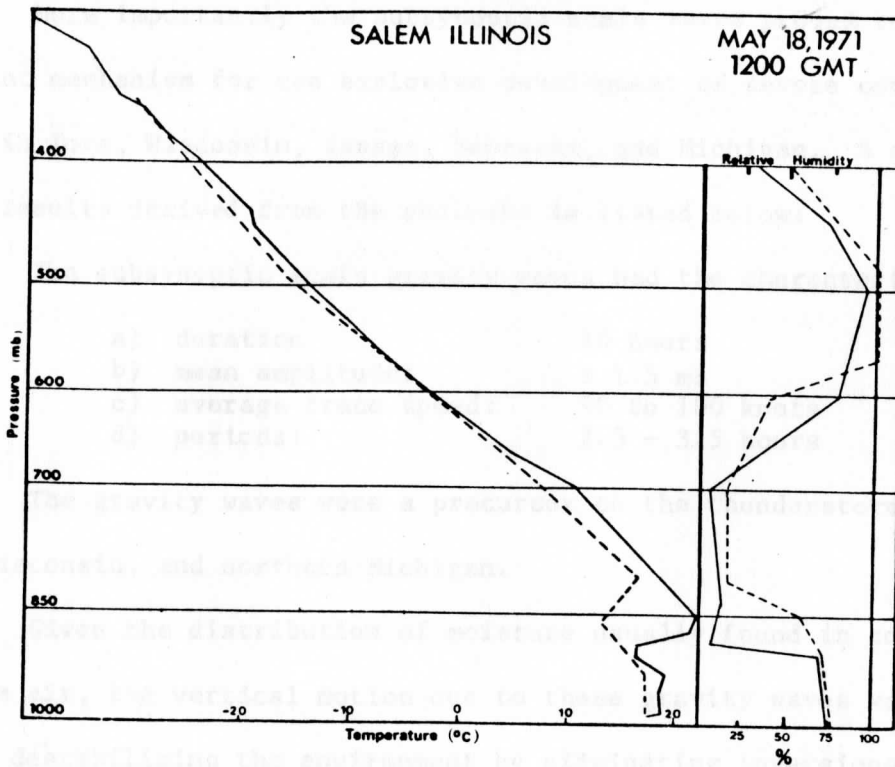
| | $W_K [850-700]$ Ergs/Gram | $W_K [850-500]$ Ergs/Gram | LPL AGW |
|-----------------------------|------------------------------|------------------------------|---------|
| Original Sounding | -6×10^5 | 5×10^5 | |
| Sounding After Gravity Wave | 8×10^5 | 3.4×10^6 | 830mb |

Figure 19a.



| | $W_k[850-700]$ Ergs/Gram | $W_k[850-500]$ Ergs/Gram | LPL AGW |
|-----------------------------|-----------------------------|-----------------------------|---------|
| Original Sounding | -1×10^5 | 2×10^6 | |
| Sounding After Gravity Wave | 0 | 3.1×10^6 | 730mb |

Figure 19b. Atmospheric soundings for Topeka, Kansas 1200 GMT May 18, 1971. See Figure 19a for entire legend.



| | $W_k[850-700]$ Ergs/Gram | $W_k[850-500]$ Ergs/Gram | LPL AGW |
|-----------------------------|-----------------------------|-----------------------------|---------|
| Original Sounding | -1×10^6 | -4.2×10^6 | |
| Sounding After Gravity Wave | -3.2×10^6 | -6.5×10^6 | none |

Figure 19c. Atmospheric soundings for Salem, Illinois 1200 GMT May 18, 1971. See Figure 19b for entire legend.

SUMMARY OF RESULTS AND SUGGESTIONS FOR FUTURE RESEARCH

This diagnostic study of the cyclogenetic period of May 18, 1971 showed that the gravity waves were an integral part of the entire system. More importantly the subsynoptic scale waves proved to be an important mechanism for the explosive development of severe convective storms in Iowa, Wisconsin, Kansas, Nebraska, and Michigan. A summary of the results derived from the analysis is listed below:

1) The subsynoptic scale gravity waves had the characteristics:

- | | |
|-------------------------|-----------------|
| a) duration: | 10 hours |
| b) mean amplitude: | ± 1.5 mb |
| c) average trace speed: | 90 to 100 knots |
| d) periods: | 2.5 - 3.5 hours |

2) The gravity waves were a precursor to the thunderstorms in Iowa, Wisconsin, and northern Michigan.

3) Given the distribution of moisture usually found in convectively unstable air, the vertical motion due to these gravity waves was capable of destabilizing the environment by eliminating inversions which act to inhibit the growth of thunderstorms. The lift was sufficient to bring parcels of saturated air to their level of free convection. Thus any small disturbance could force these parcels beyond their level of free convection and therefore initiate convection. For regions where soundings were affected in this manner, observations showed that a cause and effect relationship between the gravity waves and thunderstorms apparently existed. The passage of the trough of a wave would be followed by the reintensification of thunderstorm cells and/or the development of new cells. The heaviest precipitation usually occurred within the ridge of the wave. These observations were shown to be in very close agreement with the numerical model derived by Eom (1972).

4) The gravity waves were found to be also responsible for the three to four hour oscillation of the surface convergence fields.

Therefore, as a wave passed through a region it increased the magnitude of the surface convergence, and enhanced the development of convective systems in the process.

5) The gravity waves described above were found to exist over a large region, with all waves moving in the direction of the upper air flow. The development and movement of some of the gravity waves in regions void of any significant thunderstorms indicates an important feature of these waves. That is, the gravity waves act independently of convective systems and initiate storms only where the proper conditions exist.

While this research adds to the increasing evidence of the existence of the subsynoptic scale gravity waves and documents the consequences of these waves in convectively unstable air, there are still some important questions yet to be answered. First of all, how common is the occurrence of these waves, and secondly, to what extent are the gravity waves responsible for the initiation of severe convective storms throughout the country? Perhaps a climatological study should be undertaken to determine how often these waves occur and under which circumstances the appearance of such waves is most likely. More diagnostic studies are needed to determine the extent of the gravity wave initiation of severe convection.

This leads to the question then, what causes the gravity waves with the subsynoptic scale dimensions? The fact that significant gravity waves were found in regions void of any thunderstorms indicates that the development and movement of these waves must be due to other factors.

The features which are common to the diagnostic studies of gravity waves

(Eom 1972, Paine 1971, Matsumoto and Ninomiya 1969, Brunk 1949, Tepper 1951) are a cyclone and significant jet core. In this case study too, strong jet streaks were positioned over Texas and Kansas (Figure 2), which were also the areas where the gravity waves appeared to develop (Figure 10).

Perhaps the jet core is the key factor in the development of the gravity waves described in this and other case studies. The jet has been related to high frequency gravity waves (period less than 60 minutes - Herron and Tolstoy 1969). Cahn (1945) and Bolin (1953) have shown that gravity inertia waves, with periods on the order of hours, are also a result of the adjustment of mass near the exit region of the jet core. Therefore the jet core, which has been known to be important for cyclogenesis (Reiter 1963, Downey 1972), may also be the forcing function for the gravity waves which accompany the cyclogenetic period in this case. Additional diagnostic studies should be undertaken and numerical analysis attempted to determine if this is indeed the case.

Finally, the potential of this work for forecasting purposes remains to be explored. As it stands now it is very difficult to pinpoint gravity waves without filtering pressure traces. Yet the filtering technique employed here relies upon the use of data on either side of a point in a time series (± 3.25 hours of data required to filter pressure trace at a particular point using the filter designed for this project). Therefore this perturbation analysis is not available for real time forecasting purposes, and other methods for isolating the wave must be found. The full potential of this work can only be realized when the results of this research can be applied to forecasting the severe storms like those which ripped through the midwest on May 18, 1971.

APPENDIX: FILTERING AND MAPPING PROGRAM

written by: James E. Tear Jr.

Presented here is the computer program that was used to filter the pressure traces and plot the pressure perturbation values on mid-west base maps. The program was developed specifically for this research; however, it was designed in a general format so as to be applicable for a wide range of projects. The most impressive feature of the program is the many options which are built into it. The time interval of the series, standard deviation of the normal weight smoothing function (σ), type of filter (high and/or band pass filter) and type of output can be chosen by using the proper input statements. The program is well documented, instructing the user of the many options which are available. Below is an outline and short description of the main program and the three subroutines built into the program.

I Main Program: This section instructs the user of the options of the program and of the format of the data decks. The main program serves as the nerve center for the subroutines which calculate the weights, filters the time series, and plots the results.

II Subroutine - "Weights": This subroutine calculates the weights of the normal curve smoothing function, prints them out, and returns the weights to the Main Program. The subroutine also generates the response function for the high and/or band pass filter. The time interval, and σ must be specified for the calculation of the weights.

III Subroutine - "Filter": This subroutine simply filters a time series using the weights generated by the "Weights" subroutine, and returns filtered data to the Main Program.

IV Subroutine - "Maps": This subroutine is optional. If "Maps" is included in the specified position on the input cards (see comments in main program), midwest base maps will be printed with the filtered values plotted underneath the proper stations. Figure 20 is a base map produced by the program with all state boundaries, great lakes, and station call letters printed out. If "Maps" is not included in the data deck, a listing of the filtered values will be printed out.

Main Program for the High and Band Pass Filter

| | | |
|----------|---|----------|
| COMMENT' | EXPLANATION OF INPUT PARAMETERS AND DATA | JET00040 |
| COMMENT' | III NUMBER OF STATIONS ON THE MAP | JET00050 |
| COMMENT' | JJJ NUMBER OF DATA IN PRESSURE TIME SERIES | JET00060 |
| COMMENT' | JJJ SHOULD BE A MULTIPL ⁿ OF 10 | JET00070 |
| COMMENT' | IMAX NUMBER OF STATIONS TO BE READ IN FOR THIS RUN | JET00080 |
| COMMENT' | IMAX MUST BE LESS THAN OR EQUAL TO III | |
| COMMENT' | TSTART TIME OF FIRST PRESSURE DATUM (CST) | JET00090 |
| COMMENT' | TINT TIME INTERVAL OF PRESSURE DATA | JET00100 |
| COMMENT' | SIGH SIGMA FOR THE HIGH PASS FILTER | JET00110 |
| COMMENT' | SIGL SIGMA FOR THE LOW PASS FILTER | JET00120 |
| COMMENT' | SIGH IS GREATER THAN SIGL | JET00130 |
| COMMENT' | IQ IF IQ=0 THEN SPECS FOR FILTER ARE NOT LISTED | JET00140 |
| COMMENT' | JMAX NUMBER OF PRESSURE DATA TO READ | JET00150 |
| COMMENT' | JMAX MUST BE EQUAL TO OR LESS THAN JJJ | |
| COMMENT' | START BEGIN TIME IN HOURS FOR PRINTING OF MAPS | JET00160 |
| COMMENT' | FIN END TIME IN HOURS FOR PRINTING OF MAPS | JET00180 |
| COMMENT' | INDATE DATE OF FIRST PRESSURE DATUM | JET00200 |
| COMMENT' | FILTP 'HIGH' GIVES MAPS WITH HIGH PASS FILTER LISTED | JET00210 |
| COMMENT' | 'BAND' GIVES MAPS WITH BAND PASS FILTER LISTED | JET00220 |
| COMMENT' | MAPQ 'MAPS' GIVES PRINTING OF MAPS. OTHERWISE NO MAPS | JET00230 |
| COMMENT' | MONTH SHOULD BE MONTH AND YEAR. EX' 'MAY 1972' | JET00240 |
| COMMENT' | CALLET THREE CALL LETTERS OF THE STATION | JET00250 |
| COMMENT' | NUMSTA THE MAP PRINT CODE FOR THE STATION | JET00260 |
| COMMENT' | STANAM FULL NAME OF THE STATION | JET00270 |
| COMMENT' | P'S INPUT PRESSURE DATA | JET00280 |
| | DIMENSION PB(JJJ),IPP(III,JJJ),JK(JJJ),PH(JJJ),WH(50),P(JJJ) | JET00290 |
| | DIMENSION CALLET(III),NUMSTA(III),IDATE(JJJ),NP(III) | JET00300 |
| | DIMENSION IHOURL(JJJ),MIN(JJJ),II(III),WL(50),STANAM(III,4) | JET00310 |
| | DIMENSION MONTH(3),MTEST(3) | JET00320 |
| | DATA MTEST/1RH TEST MAP | JET00330 |
| | READ,IMAX,TSTART,TINT,SIGH,SIGL,IQ,JMAX,START,FIN,INDATE | JET00340 |
| | READ 1,FILTP,MAPQ,MONTH | JET00350 |
| 1 | FORMAT (A4,1X,A4,1X,3A6) | JET00360 |
| | CALL WEIGHT (SIGH,SIGL,WH,WL,TINT,NH,IQ) | JET00370 |
| | DO 2 J=1,JMAX | JET00380 |
| | JK(J)=J | JET00390 |
| | T=TSTART+TINT*(J-1) | JET00400 |
| | IDATE(J)=INDATE+T/24 | JET00410 |
| | DO 81 IT=1,10 | JET00420 |
| | IF (24.-T),.80 | JET00430 |
| 81 | T=T-24. | JET00440 |
| 80 | IHOURL(J)=T | JET00450 |
| | MIN(J)=(T-IHOURL(J))*60 | JET00460 |
| | DO 2 I=1,III | JET00470 |
| | NP(I)=9999 | JET00480 |
| 2 | IPP(I,J)=9999 | JET00490 |
| | DO 3 I=1,IMAX | JET00500 |
| | READ 6,CALLET(I),NUMSTA(I),(STANAM(I,J),J=1,4) | JET00510 |
| 6 | FORMAT (A3,1X,I3,1X,4A6) | JET00520 |
| | NUM=NUMSTA(I)-100 | JET00530 |
| | NP(NUM)=NUMSTA(I) | JET00540 |
| | READ 5,(P(J),J=1,JMAX) | JET00550 |
| 5 | FORMAT (5X,15F5.2) | JET00560 |
| | IF (NUM.LE.0) GO TO 90 | JET00570 |
| | IF (NUM.LE.III) GO TO 87 | JET00580 |
| 90 | CONTINUE | JET00590 |
| | IIX=III | JET00600 |
| | PRINT 88,CALLET(I),NUM,IIX | JET00610 |
| 88 | FORMAT (1H1,A3,' SKIPPED BECAUSE NUM IS',I4,'. IT SHOULD BE ' | JET00620 |
| | 2 ' BETWEEN 0 AND', I4) | JET00630 |
| | GO TO 3 | JET00640 |
| 87 | CONTINUE | JET00650 |
| | CALL FILTER (JMAX,P,PB,PH,WH,WL,NH) | JET00660 |
| | DO 91 J=1,JMAX | JET00670 |
| | PB(J)=PB(J)*.33,9 | JET00380 |
| 91 | PH(J)=PH(J)*.33,9 | JET00690 |

Main Program

{continue}

```

PRINT 4,CALLET(I),((JK(J*10+K),K=1,I),,(I*HOUR(J*10+K),MIN(J*10+K),JET00700
1 K=1,I),)
JET00710
2 (P(J*10+K),K=1,I),,(PB(J*10+K),K=1,I),),(PH(J*10+K),K=1,I),)
JET00720
3 J=0,I=20
JET00730
4 FORMAT (I1I,A3//(' INTERVAL NUMBER',4X,I0I10/' TIME',15X,I0(I7,'
JET00740
2',I2)/
JET00750
3 ' PRESSURE DATA',6X,I0F10.1/' BAND PASS FILTER',3X,I0F10.0/
JET00760
4 ' HIGH PASS FILTER',3X,I0F10.0//))
JET00770
IF (FILTY.P.NF.4H)AND) GO TO 7
JET00780
DO R J=1,JMAX
JET00790
IA=PR(J)+.5
JET00800
IF (IA.LF.0) IA=IA-1
JET00810
IPP(NUM,J)=IA
JET00820
GO TO 3
JET00830
7 IF (FILTY.P.NE.4HHIGH) GO TO 9
JET00840
DO I1 J=1,JMAX
JET00850
IA=PH(J)+.5
JET00860
IF (IA.LF.0) IA=IA-1
JET00870
IPP(NUM,J)=IA
JET00880
GO TO 3
JET00890
11 PRINT I3,FILTY
JET00900
13 FORM T (I1I,A4,' IS NOT LEGAL FOR FILTY.P.
JET00910
STOP
JET00920
3 CONTINUE
JET00930
IF (MAPQ.EQ.4HMAPS)GO TO 84
JET00940
PRINT 85,MAPC
JET00950
85 FORMAT (I1I,'MAPS NOT PRINTED BECAUSE MAPQ IS ',A3)
JET00960
STOP
JET00970
84 CONTINUE
JET00980
PRINT 89,((STANAM(I,J),J=1,4),CALLET(I),NUMSTA(I),I=1,IMAX)
JET00990
89 FORMAT (I1I9STING OF STATIONS WITH CALL LETTERS AND PRINT CODES.
JET01000
2 / (5X,4A6,5X,A3,5X,I3 )
JET01010
DO R6 I=1,I11
JET01020
JK(I)=100+I
JET01030
CALL MAP (0,MTEST ,0, 0,0,JK,FILTY)
JET01040
CALL MAP (0,MTEST ,0, 0,0,NP,FILTY)
JET01050
JB=START*4
JET01060
JE=FIN*4
JET01070
DO I0 J=JR,JF
JET01080
DO R2 I=1,I11
JET01090
I1(I)=IPP(I,J)
JET01100
83 CALL MAP (J,MONTH,DATE(J), I HOUR(J),MIN(J),I,FILTY)
JET01110
10 END
JET01120

```


Subroutine: filters time series

```

FOR IS ,FILTER
SUBROUTINE FILTER (JMAX,DATA,BAND,HPASS,WH,WL,NH)
DIMENSION DATA(JMAX),BAND(JMAX),HPASS(JMAX),WH(50),WL(50)
NHH=NH-1
JNH=JMAX-NH
DO 7 I=NH,JNH
SUL=WL(1)*DATA(I)
SUM=WH(1)*DATA(I)
DO 8 K=1,NHH
SUL=SUL+WL(K+1)*(DATA(I+K)+DATA(I-K))
SUM=SUM+WH(K+1)*(DATA(I+K)+DATA(I-K))
RAND(I)=SUL-SUM
7 HPASS(I)=DATA(I)-SUM
RETURN
END
JET03050
JET03060
JET03070
JET03080
JET03090
JET03100
JET03110
JET03120
JET03130
JET03140
JET03150
JET03160
JET03170
JET03180
JET03190

```

Subroutine: prints midwest base maps and plots filtered values

```

FOR IS ,MAP
SUBROUTINE MAP (NO,MONTH,IDATE, ITIME,MTIME,II,FILTYP)
PARAMETER NN=120
DIMENSION II(NN),MONTH(3)
PRINT 4,NO,IDATE,MONTH, ITIME,MTIME,FILTYP
4 FORMAT (11,4X,'FILTERED PRESSURES FROM PASS FILTER.',10X,
2 'MAP ',I4,',',10X,'DATE',I3,1X,3A6,T123,'0',
2 T194, 10X,'TIME',I3,')
3 I2,' CST.',T30,A4)
PRINT 1,(II(I),I=1,9)
1 FORMAT (
2 ' 2',T60,'+++' /
3 ' 3',T51,'+++++' /T87,'+++++' /T18,'ADAPTED FROM',T1,
4 ' 4',T51,'+',T63,'++++' INL',T84,10('+' ) /
5 T14,'CHART 9 WEATHER MAP',T1,
5 ' 5',T51,'+',T64,I4,'+',T82,'*QT',10('+' ) /T18,'BY JIM TEAR',
6 T1,
6 ' 6',T52,'+',T70,'+++++' /I4,16('+' ) /
7 ' 7',T52,'+',T78,22('+' ) /T10,'LAMBERT CONFORMAL PROJECTION',T1,
8 ' 8', T52,'+',T61,'*BJI',T76,24('+' ) /
9 ' 9',T13,'STANDARD PARALLELS ',T52,'+',T59,I4,T68,'*H18',
9 T74,12('+' ),'*CMX',11('+' ),T115,'*SR',T33,'AT' /
9 ' 10', T52,'+',T66,I4,3X,11('+' ) /
9 I4,14('+' ),T113,I4,T11,'25 DEG AND 48 D'G, 30 MIN' /
1 ' 11',T13,'SCALE--1 TO 7,500,000', T52,'+',T71,'*DLH ',
1 T9,'*QT',8('+' ),'*SSM',5X,'+',T76,'+++++' /
2 ' 12', T52,'+',T69,I4,6X,'+',
2 5X,I4,6X,'+',I4,14('+' ) /
3 ' 13',T22,'T1('+' ), T53,'+',4X,'*AXN',T70,'+',
3 T78,'*PKF',1X,'+',4X,'*ESC',26('+' ) /
PRINT 3,(II(I),I=10,28)
3 FORMAT (
4 ' 14', T52,'+',3X,I4,T69,'+',6X,I4,T8
4 7,'+',I4,6X,'+',*PLN+++++',4X,'+',3X,T93,6('+' ),T110,'+',
4 T118,'+',T22,'+' /
5 ' 15',T52,'+',T63,'*STC',2X,'+',T89,'+',5X,T22,'+',T98,
5 '+',I4,5X,'+',T93,'+',T46,'*ABR',T105,'APN' /
6 ' 16',T54,'+',6X,I4,4X,'+',T89,'+',3X,'+',T106,I4,4X,
6 T93,'+',T110,'+',2X,'+',T116,'*VV',T22,'+',T44,I4 /
7 ' 17',T54,'+',T67,'*MSP',3X,'*EAU',4X,'*AUW',3X,'+',
7 3X,'*TVC',T108,'+',T115,I4,T22,'+',T51,'*ATY' /
8 ' 18',T54,'+',5X,'*RWF',T65,I4,T22,'+',T49,I4,
8 T103,'*HTL',8('+' ),T69, '+',15,I8,5X,'*GRH++++',15/T71,'+',T1,
9 ' 19',T58,I4,T72,'+',T87,I4,'+',T54,'+',T106,'+',
9 T101,I4,T22,'+' /T22,'+',T1,
9 ' 20',T54,'+',T70,'*RST+LSE',T90,'+',T105,'MBS '+',
1 ' 21',T54,'+',T68,I4,I7,T90,'+',110,'* '+',T124,'+',
1 T74,'+',T22,'+' )
PRINT 6,(II(I),I=29,46)
6 FORMAT (
2 ' 22',T53,22('+' ),3X,'*LNR',7X,6('+' ),T103,I4,'*FNT','+',
2 T120,7('+' ),T22,'+',T53,'*FSD',T96,'*MKJ',T83,'*MSN' /
3 ' 23',T21,25('+' ),T53,'+',5X,'*SPC',4X,'*MCW',4X,'+',
3 I5,2X,' *MKE++ *GRR *LAN',T116,10('+' ),T45,'*PCK',16,
3 T82,I4,T94,I4,T111,'+' /
4 ' 24',T21,'+',T37,'*VTN',T46,'++++' '+',17,I8,T76,'+++++',
JET01130
JET01140
JET01150
JET01160
JET01170
JET01180
JET01190
JET01200
JET01210
JET01220
JET01230
JET01240
JET01250
JET01260
JET01270
JET01280
JET01290
JET01300
JET01310
JET01320
JET01330
JET01340
JET01350
JET01360
JET01370
JET01380
JET01390
JET01400
JET01410
JET01420
JET01430
JET01440
JET01450
JET01460
JET01470
JET01480
JET01490
JET01500
JET01510
JET01520
JET01530
JET01540
JET01550
JET01560
JET01570
JET01580
JET01590
JET01600
JET01610
JET01620
JET01630
JET01640
JET01650
JET01660
JET01670
JET01680

```

```

4 6('),I4,++++, I4,I6,4X,'*DET',11('),T43,I4/ JET01690
5 ' 25',T21,+,T35,I4,T51,++++SUX',T71,'*ALO *DBQ *RFD', JET01700
5 2X,+++++,T104,'*JXN',I5,9(')/ JET01710
6 ' 26',T21,+,T52,I4,T69,I4,I7,I7,3X,12('),I4,12(')/ JET01720
7 ' 27',T21,+,X,'*BFF',T42,'*BUB *OFK +',T74,'*CID +', JET01730
7 T91,'*MDX *SBN +',T112,++++ JET01740
PRINT 7,(I(1),I=47,63) JET01750
7 FORMAT ( JET01760
8 ' 28',T21,+,I4,T40,I4,I7,T65,'*DSM',I7,3X,+,T89,I4,I7,3X, JET01770
R '+',T5R,+/ JET01780
9 ' 29',T21,+, *SNY',T63,I4, T79,'*MLI',T92,+,10X,+, JET01790
9 T35,'*LBF',T55,'*OMA'/
' 30',T21,+,I4,++++,T46,'*GRI',I7,T71,'*OTM',2X,I4,T33,I4,
' T92,+,1X,+,T4,18(')/ JET01820
1 ' 31',T29,+, *IML',T44,I4,4X,'*LNK',T69,I4,3X,+,5X,'*PIA', JET01830
1 5X,+, *LA6',5X,+/ JET01840
2 T29,I4,T50,I4,3X,7('),*LMN',+++++,5X,I4,T92,I4,7X, JET01850
2 '+',T2,'32') JET01860
PRINT 8,(I(1),I=64,75) JET01870
R FORMAT ( JET01880
3 ' 33',T29,3C('),I7,6X,'*IRK',1X,+,T72,+,10X,+,T24,'*AKO' JET01890
/ JET01900
4 ' 34',T29,+,T59,+,T68,I4,3X,+,*UIN *SPI I,T92,+,10X,+, JET01910
4 T17,'*DEN',I5/ JET01920
5 ' 35',T29,+,*,GLD', T60,+,I74,I4,I7,T92,+,10X, JET01930
5 '+',T15,I4,3X,'*LIC',T48,'*CNK'/ JET01940
6 ' 36',T28,I4,T39,'*HLC',I7,6X,+, *MKC',T77,+,T86,'*VLA',1X, JET01950
6 '+',10X,+,T20,I4/ JET01960
7 ' 37', T37,I4,2X,'*RSL *SLN',5X,+,2X,+,I4,6X,'*CBI ' JET01970
7 *SIL',I6,4X,+,9X,+,T29,+,T54,'*TOP') JET01980
PRINT 9,(I(1),I=76,94) JET01990
9 FORMAT ( JET02000
8 ' 38',T29,+,T41,I4,3X,I4,3X,I4,2X,+,T69,I4,4X,I4, JET02010
8 T92,+,T101,+/ JET02020
9 ' 39',T17,'*PUB *LHX +',T55,'*EMP +',T80,+,T91,+, JET02030
9 6X,++++ JET02040
( ' 40',T15,I4,I5,2X,'*LAA',4X,'*GCK',T53,I4,4X,+,T74,'*VIM',2X, JET02050
( '+',8X,+++++ JET02060
1 1X, JET02070
1 '41',T24,I4,+,I6,2X,'*DDC',8X,'*ICT',4X,'*CNU',T72,I4,7X, JET02080
1 '+',6X,+,T12,'*ALS' JET02090
2 ' 42',T18,'*TAD',7X,+,6X,I4,8X,I4,4X,I4,1X,+,T84,+,4X,+, JET02100
2 T17,I4 JET02110
3 ' 43',12('),I4,42('),*JLN *SGF',T83,'*CGI +' JET02120
4 ' 44',T24,+,T50,'*PNC',6X,I4,I6,4X,'*WPS',3X,I4,+, JET02130
PRINT 10,(I(1),I=95,109) JET02140
10 FORMAT ( JET02150
5 ' 45',T23,'*CAO',11('),T48,I4,9X,11('),I4,7('),3X,+, JET02160
6 ' 46',T21,I4,T37,+,*GAG',T56,*TUL +',T80,'*JBR +'/ JET02170
7 ' 47',T14,'*LV5',6X,+, *DHT',8Y,I4,T54,I4,3X,+, *FVY',T78,I4, JET02180
7 +',T37,+,T6,'*SAF+' JET02190
8 ' 48',T12,I4,8X,+,I4,8X,+,T61,+,I4,T84,+,T6,I4 JET02200
9 ' 49',T20,'*TCC+ *AMA +',T48,'*OKC',9X,+, *FSM',T83,+, JET02210
9 T7,'*ABO' JET02220
/ ' 50',T18,I4,2X,+,I6,6X,+, *HBR',I5,6X,'*MLC +',I4,T82,+, JET02230
/ T5,I4 JET02240

PRINT 11,(I(1),I=110,116) JET02250
11 FORMAT ( JET02260
1 ' 51',T24,+,T37,+,I5,T54,I4,4X,+,T72,'*LIT',5X,+, JET02270
2 ' 52',T24,+,T36,'*CDS',+,T62,+,7X,I4,6X,+, JET02280
3 ' 53',T24,+,9X,I4,4X,7('),T62,+,T79,+, JET02290
4 ' 54',T24,+, *LBB',T44,'*SPS',15('),T78,+, JET02300
5 ' 55',T16,'*ROW',4X,+,I4,T42,I4,T63,++++,T78,+, JET02310
6 ' 56',T14,I4,6X,+,T65,+,T78,+, JET02320
7 ' 57',T56,'*QSW *',4X,I4(+) JET02330
5 CONTINUE JET02340
END JET02350

```

map subroutine
{continue}

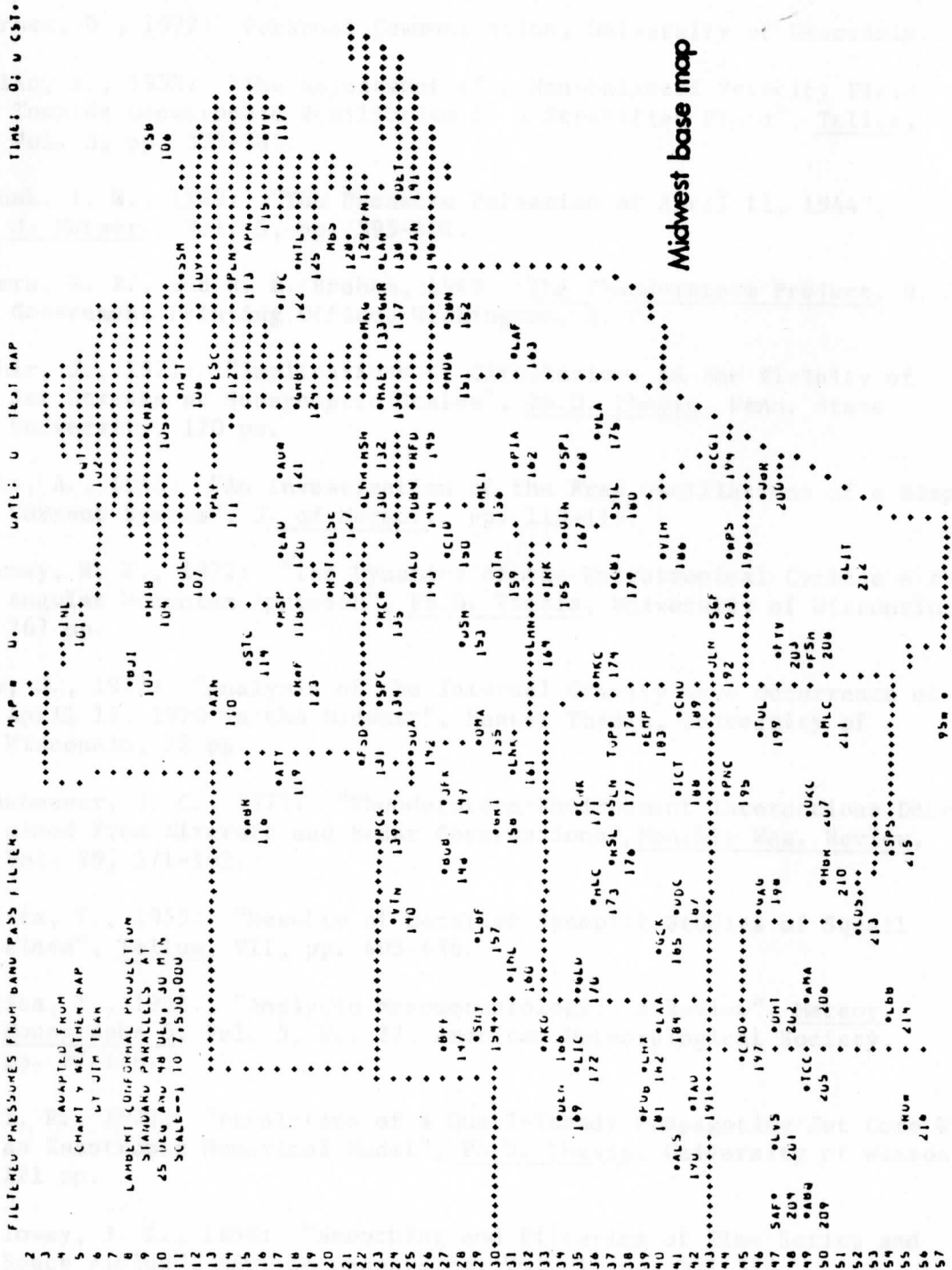


Figure 20. Midwest base map produced by the computer program.

BIBLIOGRAPHY

- Auvine, B. A., 1970: "A Study of the Interaction of Satellite and Surface Observations in a Severe Local Storm Situation", Master of Science Thesis, University of Wisconsin, 38 pp.
- Barber, D., 1972: Personal Communication, University of Wisconsin.
- Bolin, B., 1953: "The Adjustment of a Non-balanced Velocity Field Towards Geostrophic Equilibrium in a Stratified Fluid", Tellus, Vol. 3, pp. 373-385.
- Brunk, I. W., 1949: "The Pressure Pulsation of April 11, 1944", J. Meteor., Vol. 5, pp. 395-401.
- Byers, H. R., and R. R. Braham, 1949: The Thunderstorm Project, U. S. Government Printing Office, Washington, D. C.
- Cahir, J., 1971: "Implications of Circulations in the Vicinity of Jet Streaks at Subsynoptic Scales", Ph.D. Thesis, Penn. State University, 170 pp.
- Cahn, A., 1945: "An Investigation of the Free Oscillations of a Simple Current System", J. of Meteor., pp. 113-119.
- Downey, W. K., 1972: "The Dynamics of the Extratropical Cyclone - An Angular Momentum Approach", Ph.D. Thesis, University of Wisconsin, 267 pp.
- Eom, J., 1972: "Analysis of the Internal Gravity Wave Occurrence of April 19, 1970 in the Midwest", Master Thesis, University of Wisconsin, 72 pp.
- Fankhauser, J. C., 1971: "Thunderstorm-Environment Interactions Determined From Aircraft and Radar Observations", Monthly Wea. Review, Vol. 99, 171-192.
- Fujita, T., 1955: "Results of Detailed Synoptic Studies of Squall Lines", Tellus, VII, pp. 405-436.
- Fujita, T., 1963: "Analytic Mesometeorology: A Review", Meteor. Monographs 5, Vol. 5, No. 27, American Meteorological Society, pp. 77-128.
- Gall, R., 1972: "Prediction of a Quasi-Steady Propagating Jet Core With an Isentropic Numerical Model", Ph.D. Thesis, University of Wisconsin, 121 pp.
- Holloway, J. L., 1958: "Smoothing and Filtering of Time Series and Space Fields", Adv. in Geophysics, Vol. 4, pp. 351-389.

- Herron, J. J., and I. Tolstoy, 1969: "Tracking Jet Stream Winds From Ground Level Pressure Signals", JAS, Vol. 26, pp. 266-269.
- Ludlum, F. H., 1963: "Severe Local Storms: A Review", Meteor. Monographs 5, Vol. 5, No. 27, American Meteorological Society, pp. 1-30.
- Matsumoto, S., K. Ninomiya, and T. Akiyama, 1967: "A Synoptic and Dynamic Study on the Three Dimensional Structure of Mesoscale Disturbances Observed in the Vicinity of a Cold Vortex Center", J. of the Meteor. Soc. of Japan, Vol. 45, No. 1, pp. 64-81.
- Matsumoto, S., and T. Akiyama, 1969 A: "Some Characteristic Features of the Heavy Rainfalls Observed Over Western Japan on July 9, 1967, Part 1: Mesoscale Structure and Short Period Pulsation", J. of the Meteor. Soc. of Japan, Vol. 47, No. 4, pp. 255-266.
- Matsumoto, S., and Y. Tsuneoka, 1969 B: "Some Characteristic Features of the Heavy Rainfalls Observed Over the Western Japan on July 9, 1967, Part 2: Displacement and Life Cycle of Mesoscale Rainfall Cells", J. of the Meteor. Soc. of Japan, Vol 47, No. 4, pp. 267-278.
- Matsumoto, S., and K. Ninomiya, 1969: "On the Role of Convective Momentum Exchange in the Mesoscale Gravity Wave", J. of the Meteor. Soc. of Japan, Vol 47, No. 2, pp. 75-85.
- Miller, R. C., 1967: "Notes on Analysis and Severe Storm Forecasting Procedures of the Military Weather Warning Center", Air Weather Service (MAC) U. S. Air Force, Technical Report No. 200.
- Miller, R. C., A. Bidner, and R. A. Maddox, 1971: "The Use of Computer Products in Severe Weather Forecasting (The Sweat Index)", Preprints of Papers Presented at the Seventh Conference on Severe Local Storms, AMS Unpublished Manuscript, pp. 1-6.
- National Severe Storms Project, (U. S. Weather Bureau), 1963: "Environmental and Thunderstorm Structures as Shown by National Severe Storms Project Observations in Spring 1960 and 1961", Monthly Weather Review, Vol. 91, No. 6, pp. 271-292.
- Newton, C. W., 1963: "Dynamics of Severe Convective Storms", Meteor. Monographs 5, Vol. 5, No. 27, American Meteorological Society, pp. 33-55.
- Ninomiya, K., 1969: "Meteorological Satellite Study on the Development of Tornado Producing Thunderstorms", Preprints of Papers Presented at the Sixth Conference on Severe Local Storms, AMS Unpublished Manuscript, pp. 202-207.
- Paine, D. A., and M. L. Kaplan, 1971: "The Linking of Multiscaled Energy Sources Creating a Severe Local Winter Storm", Preprints of Papers Presented at the Seventh Conference on Severe Local Storms, AMS Unpublished Manuscript, pp. 297-306.

- Reiter, E. R., 1963: Jet Stream Meteorology, The University of Chicago Press, Chicago Illinois, Chapter 6, pp. 324-372.
- Schlesinger, R. E., 1971: "A Numerical Model of Deep Moist Convection: The Influence of Ambient Conditions and Internal Physical Mechanisms, "Studies of the Atmosphere Using Aerospace Probing/Annual Report, Vol. 1", Space Science and Engineering Center, University of Wisconsin, pp. 149-356.
- Stadjuhar, R. E., 1970: "Dynamic Destabilization and Squall Line Formation", Master of Science Thesis, University of Wisconsin. 38 pp.
- Storm Data, May 1971: U. S. Department of Commerce, Vol. 13, No. 5.
- Tepper, M., 1950" "A Proposed Mechanism of Squall Lines: The Pressure Jump Line", J. of Meteor., Vol. 7, pp. 21-29.
- Tepper, M., 1951: "On the Desiccation of a Cloud Bank by a Propagated Pressure Wave", Monthly Wea. Review, Vol. 79, No. 4, pp. 61-70.
- Tepper, M., 1954: "Pressure Jump Lines in Midwestern United States, January-August 1951", Research Paper No. 37, United States Weather Bureau, Washington, D. C., 70 pp.
- Uccellini, L. W., 1971: "Surface Divergence and Convergence Fields Associated With Midwestern Convective Systems", B.S. Thesis, Dept. of Meteorology, University of Wisconsin, Unpublished Manuscript, 61 pp.